Title: Tree height and leaf drought tolerance traits shape growth responses across droughts in a temperate broadleaf forest

Authors: Ian R. McGregor[1,2], Ryan Helcoski[1], Norbert Kunert[1,3], Alan J. Tepley[1,4], Erika B. Gonzalez-Akre[1], Valentine Herrmann[1], Joseph Zailaa[1,5], Atticus E.L. Stovall[1,6,7], Norman A. Bourg[1], William J. McShea[1], Neil Pederson[8], Lawren Sack[9,10], Kristina J. Anderson-Teixeira[1,3]*

Author Affiliations:

1. Conservation Ecology Center; Smithsonian Conservation Biology Institute; National Zoological Park, Front Royal, VA 22630, USA
2. Center for Geospatial Analytics; North Carolina State University; Raleigh, NC 27607, USA
3. Center for Tropical Forest Science-Forest Global Earth Observatory; Smithsonian Tropical Research Institute; Panama, Republic of Panama
4. Canadian Forest Service, Northern Forestry Centre, Edmonton, Alberta, Canada T6H 3S5
5. Biological Sciences Department; California State University; Los Angeles, CA 90032, USA
6. Department of Environmental Sciences, University of Virginia, Charlottesville, VA 22903, USA
7. NASA Goddard Space Flight Center; Greenbelt, MD 20771, USA
8. Harvard Forest, Petersham, MA 01366, USA
9. Department of Ecology and Evolutionary Biology; University of California, Los Angeles; Los Angeles, CA 90095, USA
10. Institute of the Environment and Sustainability; University of California, Los Angeles; Los Angeles, CA 90095, USA

*corresponding author: teixeirak@si.edu; +1 540 635 6546

Received: *24 July 2020*

Accepted: *2 October 2020*

This article has been accepted for publication and undergone full peer review but has not been through the copyediting, typesetting, pagination and proofreading process, which may lead to differences between this version and the Version of Record. Please cite this article as doi: 10.1111/nph.16996

Summary

- As climate change drives increased drought in many forested regions, mechanistic understanding of the factors conferring drought tolerance in trees is increasingly important. The dendrochronological record provides a window through which we can understand how tree size and traits shape growth responses to droughts.
- We analyzed tree-ring records for twelve species in a broadleaf deciduous forest in Virginia (USA) to test hypotheses for how tree height, microenvironment characteristics, and species' traits shaped drought responses across the three strongest regional droughts over a 60-year period.
- Drought tolerance (resistance, recovery, and resilience) decreased with tree height, which was strongly correlated with exposure to higher solar radiation and evaporative demand. The potentially greater rooting volume of larger trees did not confer a resistance advantage, but marginally increased recovery and resilience, in sites with low topographic wetness index. Drought tolerance was greater among species whose leaves lost turgor (wilted) at more negative water potentials and experienced less shrinkage upon desiccation.
- The tree-ring record reveals that tree height and leaf drought tolerance traits influenced growth responses during and after significant droughts in the meteorological record. As climate change-induced droughts intensify, tall trees with drought-sensitive leaves will be most vulnerable to immediate and longer-term growth reductions.

Key words: annual growth; crown exposure; drought; Forest Global Earth Observatory (ForestGEO); leaf drought tolerance traits; temperate broadleaf deciduous forest; tree height; tree-ring

Introduction

Forests play a critical global role in climate regulation (Bonan 2008), yet there remains enormous uncertainty as to how the forest-dominated terrestrial carbon sink will respond to climate change (Friedlingstein et al. 2006). An important aspect of this uncertainty lies with physiological responses of trees to drought (Kennedy et al. 2019). In many forested regions around the world, the risk of severe drought is increasing (Trenberth et al. 2014; Dai, Zhao, and Chen 2018), often despite increasing precipitation (Intergovernmental Panel on Climate Change 2015; Cook, Ault, and Smerdon 2015). Droughts, intensified by climate change, have been affecting forests worldwide and are expected to continue as an important driver of forest change (Allen et al. 2010; Allen, Breshears, and McDowell 2015; McDowell et al. 2020). Understanding forest responses to drought requires elucidation of how tree size, microenvironment, and species' traits jointly influence individual-level drought tolerance, defined here as a tree's ability to maintain growth during drought (*resistance*), increase growth relative to drought minimum (*recovery*), and re-establish its pre-drought growth rate (*resilience*; Lloret, Keeling, and Sala 2011). Survival has been shown to be linked to resistance, recovery, and resilience (DeSoto et al. 2020; Gessler et al. 2020), implying they may be influenced by the same factors. However, it has proven difficult to resolve the many factors affecting tree growth during drought and the extent to which their influence is consistent across droughts. This is because available forest census data only rarely captures extreme drought, whereas tree-ring records capture multiple droughts but typically focus on only the largest individuals of one or a few species.

Many studies have shown that within and across species, large trees tend to be more affected by drought. Greater growth reductions (*i.e.*, lower drought resistance) in larger trees were first shown on a global scale by Bennett et al. (2015), and subsequent studies have reinforced this finding (*e.g.*, Pretzsch, Schütze, and Biber 2018; Gillerot et al. 2020). Although lower recovery and resilience of larger trees have also been observed (Gillerot et al. 2020), results were mixed (Merlin et al. 2015), and a recent physiological model suggests that large trees destined to die following drought may still exhibit high recovery and resilience (Trugman et al. 2018). Thus, in

general we have much more limited understanding of how and why drought resilience scales with tree size.

Moreover, it has yet to be resolved which of several potential underlying mechanisms most strongly shape these trends in drought response. First, tree height itself may be a primary driver. Taller trees face the biophysical challenge of lifting water greater distances against the effects of gravity and friction (McDowell et al. 2011; McDowell and Allen 2015; Ryan, Phillips, and Bond 2006; Couvreur et al. 2018). Vertical gradients in stem and leaf traits–including smaller and thicker leaves (higher leaf mass per area), greater resistance to hydraulic dysfunction (*i.e.*, more negative water potential at 50% loss of hydraulic conductivity, more negative P50), and the tapering of hydraulic conductivity at greater heights (Couvreur et al. 2018; Koike et al. 2001; McDowell et al. 2011)–enable trees to become tall (Couvreur et al. 2018). Greater stem capacitance (*i.e.*, water storage capacity) of larger trees may also confer resistance to transient droughts (Phillips et al. 2003; Scholz et al. 2011). Taller trees have wider conduits in the basal portions of taller trees, both within and across species (Olson et al. 2018; Liu et al. 2019) and throughout the conductive systems of angiosperms (Zach et al. 2010; Olson et al. 2014, 2018), which help maintain constant the resistance that would otherwise increase as trees grow taller. Wider xylem conduits plausibly make large trees more vulnerable to embolism during drought (Olson et al. 2018), and traits conducive to efficient water transport may also lead to poor ability to recover from or re-route water around embolisms (Roskilly et al. 2019).

Larger trees may also have lower drought tolerance because of microenvironmental and ecological factors. Their crowns tend to occupy more exposed canopy positions, which are associated with higher evaporative demand (Kunert et al. 2017). Counteracting the liabilities associated with tall height, large trees tend to have larger root systems (Enquist and Niklas 2002; Hui et al. 2014), potentially mitigating some of the biophysical challenges they face by allowing greater access to water. Larger root systems–if they grant access to deeper water sources–would be particularly advantageous in drier microenvironments (e.g., hilltops, as compared to valleys and streambeds) during drought. Finally, tree size-related responses to

drought can be modified by species' traits and their distribution across size classes (Meakem et al. 2018; Liu et al. 2019). Understanding the mechanisms driving the greater relative growth reductions of larger trees during drought requires disentangling the interactive effects of height and associated exposure, root water access, and species' traits.

Debates have also arisen regarding the traits influencing tree growth responses to drought. Studies within temperate broadleaf forests have observed ring-porous species showing higher drought tolerance than diffuse-porous species (Friedrichs et al. 2009; Elliott et al. 2015; Kannenberg et al. 2019). However, this differentiation is not universal within the biome (Martin-Benito and Pederson 2015), does not hold in the global context (Wheeler, Baas, and Rodgers 2007; Olson et al. 2020), and does not resolve differences among the many species within each category. Commonly-measured traits including wood density (WD) and leaf mass per area (LMA) have been linked to drought responses within some temperate deciduous forests (Abrams 1990; Guerfel et al. 2009; Hoffmann et al. 2011; Martin-Benito and Pederson 2015) and across forests worldwide (Greenwood et al. 2017). However, in other cases these traits could not explain drought tolerance (e.g., in a tropical rainforest; Maréchaux et al. 2020), or the direction of response was not always consistent. For instance, higher wood density has been associated with greater drought resistance at a global scale (Greenwood et al. 2017), but correlated negatively with tree performance during drought in a broadleaf deciduous forest in the southeastern United States (Hoffmann et al. 2011). Thus, the perceived influence of these traits on drought resistance may actually reflect indirect correlations with other traits that more directly drive drought responses (Hoffmann et al. 2011).

In contrast, hydraulic traits have direct physiological linkages to tree growth and mortality responses to drought. For instance, water potentials at which the percent loss of conductivity surpasses a certain threshold (e.g., P50 and P88, representing 50 and 88% loss of conductivity, respectively) and hydraulic safety margin (*i.e.*, difference between typical minimum water potentials and P50 or P88) correlate with drought performance across global forests (Anderegg et al. 2016). However, these are time-consuming to measure and therefore often infeasible for predicting or modeling drought responses in highly diverse forests (*e.g.*, in the tropics). More

easily-measurable leaf drought tolerance traits that have direct linkage to plant hydraulic function can explain variation in plant distribution and function (Medeiros et al. 2019). These include leaf area shrinkage upon desiccation (PLA_{dry}; Scoffoni et al. 2014) and the leaf water potential at turgor loss point (π_{tlp}), *i.e.,* the water potential at which leaf wilting occurs (Bartlett et al. 2016a; Zhu et al. 2018). Both traits correlate with hydraulic vulnerability and drought tolerance as part of unified plant hydraulic systems (Scoffoni et al. 2014; Bartlett et al. 2016a; Zhu et al. 2018; Farrell, Szota, and Arndt 2017). The abilities of both PLA_{dry} and π_{tlp} to explain the drought tolerance of tree growth remains untested (but see Powers et al. 2020 for π_{tlp} link to mortality).

Here, we examine how tree height, microenvironment characteristics, and species' traits collectively shape three metrics of drought tolerance: (1) resistance, defined as the ratio of annual stem growth in a drought year to that which would be expected in the absence of drought from previous growth; (2) recovery, defined as the ratio of post-drought growth to growth during the drought year; and (3) resilience, defined as the ratio of post-drought to pre-drought growth (Lloret, Keeling, and Sala 2011). We test a series of hypotheses and associated specific predictions (Table 1) based on the combination of tree-ring records from the three strongest droughts over a 60-year period (1950 - 2009), species trait measurements, and census and microenvironmental data from a large forest dynamics plot in Virginia, USA. First, we focus on how tree size, alone and in its interaction with microenvironmental gradients, influences drought tolerance. We examine the contemporary relationship between tree height and microenvironment, including growing season meteorological conditions and crown exposure. We then test whether, consistent with most forests globally, larger-diameter, taller trees tend to have lower drought tolerance in this forest, which is in a region (eastern North America) represented by only two studies in the global review of (Bennett et al. 2015). We also test for an influence of potential access to available soil water, which should be greater for larger trees in dry but not in consistently wet microsites. Finally, we focus on the role of species' traits, testing the hypothesis that species' traits-–particularly leaf drought tolerance traits-–predict drought tolerance. We test predictions that drought tolerance is higher in ring-porous

than semi-ring and diffuse-porous species and that it is correlated with wood density–either positively (Greenwood et al. 2017) or negatively (Hoffmann et al. 2011) and positively correlated with LMA. We further test predictions that species with low PLA_{dry} and those whose leaves lose turgor at lower water potentials (more negative π_{tlp}) have higher tolerance.

Materials and Methods

Study site and microclimate

Research was conducted at the 25.6-ha ForestGEO (Forest Global Earth Observatory) study plot at the Smithsonian Conservation Biology Institute (SCBI) in Virginia, USA (38°53'36.6"N, 78°08'43.4"W, elevation 273-338 m above sea level (asl); Fig. **S1**) (Bourg et al. 2013; Anderson-Teixeira, Davies, et al. 2015). Climate is humid temperate, with mean annual temperature of 12.7 ∘ C and precipitation of 1005 mm yr^{-1} during our study period (1960-2009; source: CRU TS v.4.01; Harris et al. 2014). Dominant tree taxa within this secondary forest include *Liriodendron tulipifera*, oaks (*Quercus* spp.), and hickories (*Carya* spp.; Table 2).

Identifying drought years

We identified the three largest droughts within the time period 1960-2009, defining drought (Slette et al. 2019) based on Palmer Drought Severity Index (PDSI) during May-August (MJJA; Table S1), which were identified by Helcoski et al. (2019) as the months to which annual tree growth was most sensitive at this site. PDSI divisional data for Northern Virginia were obtained in December 2017 from NOAA (https://www7.ncdc.noaa.gov/CDO/CDODivisionalSelect.jsp), from which we determined the three strongest droughts during the study period occurred in 1966, 1977, and 1999 (Figs. **1, S1**; Table S1).

The droughts differed in intensity and antecedent moisture conditions (Fig. **S1**, Table S1). The 1966 drought was preceded by two years of moderate drought during the growing season and severe to extreme drought starting the previous fall. In August 1966, $PDSI$ reached its lowest monthly value (-4.82) of the three droughts. The 1977 drought was the least intense throughout the growing season, and it was preceded by 2.5 years of near-normal conditions, making it the

mildest of the three droughts. The 1999 drought was preceded by wetter than average conditions until the previous June, but *PDSI* plummeted below -3.0 in October 1998 and remained below this threshold through August 1999. Following all three droughts, *PDSI* rebounded to near-normal conditions in September or October (Fig. **S1**).

Data collection and preparation

Within or just outside the ForestGEO plot, we collected data on a suite of variables including tree heights, microenvironment characteristics, and species traits (Table 3). The SCBI ForestGEO plot was censused in 2008, 2013, and 2018 following standard ForestGEO protocols, whereby all free-standing woody stems $\geq$ 1cm diameter at breast height (DBH) were mapped, tagged, measured at DBH, and identified to species (Condit 1998). From these census data, we used measurements of DBH from 2008 to calculate historical DBH and data for all stems $\geq$ 10cm to analyze functional trait composition relative to tree height (all analyses described below).

We analyzed tree-ring data (xylem growth increment) from 571 trees representing the twelve dominant species (Table 2; Fig. **S2**). Selected species were those with the greatest contributions to woody aboveground net primary productivity ($ANPP_{stem}$) and together comprised 97% of study plot $ANPP_{stem}$ between 2008 and 2013 (Helcoski et al. 2019). Cores (one per tree) were collected within the ForestGEO plot at breast height (1.3m) in 2010-2011 or 2016-2017. In 2010-2011, cores were collected from randomly selected live trees of each species that had at least 30 individuals $\geq$ 10 cm DBH (Bourg et al. 2013). In summers of 2016 and 2017, cores were collected from all trees found to have died within the preceding year based on annual tree mortality censuses (Gonzalez-Akre et al. 2016). It is unlikely that drought was a factor in the death of any of these trees, as monthly May-Aug *PDSI* did not drop below -1.75 (near-normal) in these years or the three years prior (2013-2017). Moreover, the trees analyzed here lived at least 17-18 years past the most recent major drought (1999), whereas the meta-analysis of Trugman et al. (2018) indicates that >10-year lags in drought-attributed mortality are rare. Having found that trees cored dead displayed similar climate sensitivity to trees cored live

(Helcoski et al. 2019), we pooled the samples for this analysis. Cores were sanded, measured, and crossdated using standard procedures, as detailed in (Helcoski et al. 2019). The resulting chronologies (Fig. **1a**) were published in Zenodo (Gonzalez-Akre et al. 2019).

For each cored tree, we combined tree-ring records and allometric equations of bark thickness to reconstruct DBH for the years 1950-2009. Prior DBH was estimated using the following equation:

$$DBH_Y = DBH_{2008} - 2 * \left[r_{bark,2008} - r_{bark,Y} + \sum_{year=Y}^{2008} r_{ring,Y} \right]$$

Here, Y denotes the year of interest, r_{ring} denotes ring width derived from cores, and r_{bark} denotes bark thickness, which was estimated from species-specific allometries based on the bark thickness data from the site (Table S2; Anderson-Teixeira, McGarvey, et al. 2015).

Tree heights (H) were measured by several researchers for a variety of purposes between 2012 and 2019 (n=1,518 trees). Methods included direct measurements using a collapsible measurement rod on small trees (NEON 2018) or a tape measure on recently fallen trees (this study); geometric calculations using clinometer and tape measure (Stovall, Anderson-Teixeira, and Shugart 2018b) or digital rangefinders (Anderson-Teixeira, McGarvey, et al. 2015; NEON 2018); and ground-based LiDAR (Stovall, Anderson-Teixeira, and Shugart 2018a). Rangefinders used either the tangent method (Impulse 200LR, TruPulse 360R) or the sine method (Nikon ForestryPro) for calculating heights. Both methods are associated with some error (Larjavaara and Muller-Landau 2013), but in this instance there was no clear advantage of one or the other. Species-specific height allometries were developed using log-log regression ($ln[H] \sim ln[DBH]$; Table S3). For species with insufficient height data to create reliable species-specific allometries (n=2, *Juglans nigra* (JUNI) and *Fraxinus americana* (FRAM)), heights were calculated from an equation developed by combining the height measurements across all species. We then used these allometries to estimate H for each drought year, Y, based on reconstructed DBH_Y (Fig. **S3**).

To characterize how environmental conditions vary with height, data were obtained from the NEON tower located <1km from the study area via the neonUtilities package (Lunch et al. 2020). We used wind speed, relative humidity, and air temperature data, all measured over a vertical profile spanning heights from 7.2 m to above the top of the tree canopy (31.0 or 51.8m, depending on censor), for the years 2016-2018 (NEON 2018). After filtering for missing and outlier values, we determined the daily minima and maxima, which we then aggregated at the monthly scale.

Crown position–a categorical variable classifying trees based on exposure to sunlight–was recorded for all cored trees that remained standing during the growing season of 2018 following the protocol of Jennings, Brown, and Sheil (1999). Trees were classified as follows: *dominant* trees were defined as those with crowns above the general level of the canopy, *co-dominant* trees as those with crowns within the the canopy; *intermediate* trees as those with crowns below the canopy level, but illuminated from above; and *suppressed* as those below the canopy and receiving minimal direct illumination from above.

Topographic wetness index (TWI), used here as a metric of long-term mean moisture availability, was calculated using the dynatopmodel package in R (Fig. **S2**) (Metcalfe, Beven, and Freer 2018). Originally developed by Beven and Kirkby (1979), TWI was part of a hydrological run-off model and has since been used for a number of purposes in hydrology and ecology (Sørensen, Zinko, and Seibert 2006). TWI calculation depends on an input of a digital elevation model [DEM; ~3.7 m resolution from the elevatr package (Hollister 2018), and from this yields a quantitative assessment defined by how "wet" an area is, based on areas where run-off is more likely. From our observations in the plot, TWI performed better at categorizing wet areas than the Euclidean distance from the stream.

Species' trait data were collected in August 2018 (Tables 2-3; Fig. **S4**). We sampled small, sun-exposed branches up to eight meters above the ground from three individuals of each species in and around the ForestGEO plot. Sampled branches were re-cut under water at least two nodes above the original cut and re-hydrated overnight in covered buckets under opaque plastic bags before measurements were taken. Rehydrated leaves taken towards the apical end of the

branch (n=3 per individual: small, medium, and large) were scanned, weighed, dried at 60 ° C for $\geq$ 48 hours, and then re-scanned and weighed. Leaf area was calculated from scanned images using the LeafArea R package (Katabuchi 2019). LMA was calculated as the ratio of leaf dry mass to fresh area. PLA_{dry} was calculated as the percent loss of area between fresh and dry leaves. WD was calculated for ~1cm diameter stem samples (bark and pith removed) as the ratio of dry weight to fresh volume, which was estimated using Archimedes' displacement. We used the rapid determination method of Bartlett et al. (2012) to estimate osmotic potential at turgor loss point (π_{tlp}). Briefly, two 4 mm diameter leaf discs were cut from each leaf, tightly wrapped in foil, submerged in liquid nitrogen, perforated 10-15 times with a dissection needle, and then measured using a vapor pressure osmometer (VAPRO 5520, Wescor, Logan, UT, USA). Osmotic potential (π_{osm}) given by the osmometer was used to estimate (π_{tlp}) using the equation $\pi_{tlp} = 0.832\pi_{osm}^{-0.631}$ (Bartlett et al. 2012).

Statistical Analysis

For each drought year, we calculated metrics of drought resistance (Rt), recovery (Rc), and resilience (Rs), following Lloret, Keeling, and Sala (2011). These metrics compare ratios of basal area increment (BAI; *i.e.*, change in cross-sectional area) before, during, and after the drought year, as specified in Table 3.

For all metrics, values <1 and >1 indicate growth reductions and increases, respectively.

Because these metrics could potentially be biased by directional pre-drought growth trends, we also tried an intervention time series analysis (ARIMA, Hyndman et al. 2020) that predicted mean drought-year growth based on trends over the preceding ten years and used this value in place of the five-year mean in calculations of resistance (Rt_{ARIMA}= observed BAI/ predicted BAI). Rt and Rt_{ARIMA} were strongly correlated (Fig. **S5**), and showed similar responses to the independent variables of interest (cf. Tables S4-55, S8-S9). Visual review of the individual tree-ring sequences with the largest discrepancies between these metrics revealed that Rt was less prone to unreasonable estimates than Rt_{ARIMA}. We therefore determined that use of 5-year

means, as described above, were more appropriate metrics than those based on ARIMA projections.

Analyses focused on testing the predictions presented in Table 1 with Rt (or Rt_{ARIMA}), Rc, or Rs as the response variable. Models were run for all drought years combined and for each drought year individually. The general statistical model for hypothesis testing was a mixed effects model, implemented in the lme4 package in R (Bates et al. 2019). In the multi-year model, we included a random effect of tree nested within species and a fixed effect of drought year to represent the combined effects of differences in drought characteristics. Individual year models included a random effect of species. All models included fixed effects of independent variables of interest (Tables 1,3) as specified below. All variables across all best models had variance inflation factors between 1 and 1.045. We used Akaike information criterion with correction for small sample sizes (AICc; see Brewer, Butler, and Cooksley 2016) to assess model selection, and conditional/marginal R-squared to assess model fit as implemented in the AICcmodavg package in R (Mazerolle and Dan Linden. 2019). Individual model terms were considered significant when their addition to a model improved fit at $\Delta\text{AICc} \geq 2.0$, where ΔAICc is the difference in AICc between models with and without the trait.

To avoid over-fitting models with five species traits (Table 3) across only 12 species, we did not include all traits as fixed effects in a single linear mixed model, but rather conducted individual tests of each species trait to determine the relative importance and appropriateness for inclusion in the main model. These tests followed the model structure specified above, with $ln[H]$ and $ln[TWI]$ added to create a base model against which we tested traits. Trait variables were considered appropriate for inclusion in the main model if their addition to the base model significantly improved fit for at least one metric of drought tolerance (Rt, Rc, or Rs; Tables S4,S6-S7). Although we tested xylem porosity as a predictor (Table 1), we did not consider it appropriate for inclusion in the main model because of its highly uneven distribution of species across categories (Table 2). In addition, we observed opposite drought responses of the only two diffuse-porous species (see Results), themselves likely representing the most and least shade-tolerant species in the study area.

We then determined the top full models for predicting each dependent variable. To do so, we compared models with all possible combinations of candidate variables, including $ln[H]$* $ln[TWI]$ and species traits as specified above. We identified the full set of models within Δ AICc=2 of the best model (that with lowest AICc). When a variable appeared in all of these models and the sign of the coefficient was consistent across models, we viewed this as support for the acceptance/rejection of the associated prediction (Table 1). If the variable appeared in some but not all of these models, and its sign was consistent across models, we considered this partial support/rejection.

All analysis beyond basic data collection was performed using R version 3.6.2 (R Core Team 2019). Other R-packages used in analyses are listed in the Supplementary Information (Methods S1).

Results

Tree height and microenvironment

In the years for which we have vertical profiles in climate data (2016-2018), taller trees–or those in dominant crown positions– were generally exposed to higher evaporative demand during the peak growing season months (May-August; Fig. **2**). Specifically, maximum daily wind speeds were significantly higher above the top of the canopy (40-50m) than within and below (10-30m) (Fig. **2a**). Relative humidity was also somewhat lower during June-August, ranging from ~50-80% above the canopy and ~60-90% in the understory (Fig. **2b**). Air temperature did not vary consistently across the vertical profile (Fig. **2c**).

Crown position varied as expected with height (dominant > co-dominant > intermediate > suppressed), but with substantial variation (Fig. **2d**). There were significant differences in height across all crown position classes (Fig. **2d**). A comparison test between height and crown position data from the most recent ForestGEO census (2018) revealed a correlation of 0.73.

Community-level drought responses

At the community level, cored trees showed substantial growth reductions in all three droughts, with a mean Rt of 0.86 in 1966 and 1999, and 0.84 in 1977 (Fig. **1b**). Across the entire study period (1950-2009), the focal drought years were the three years with the largest fraction of trees exhibiting $Rt \leq 0.7$. Specifically, in each drought, roughly 30% of the cored trees had growth reductions of $\geq$ 30% ($Rt \leq 0.7$): 29% in 1966, 32% in 1977, and 27% in 1999. However, some individuals exhibited increased growth, *i.e.*, $Rt > 1.0$: 26% of trees in 1966, 22% in 1977, and 26% in 1999. Recovery was generally strong and complete within five years following each of the drought years, with Rc averaging 1.55 in 1966, 1.42 in 1977, and 1.34 in 1999 (Fig. **S6**) and Rs averaging 1.28 in 1966, 1.19 in 1977, and 1.12 in 1999 (Fig. **1c**).

In the context of the multivariate models, all response variables varied across drought years. That is, in models with all drought years combined, year was present in all of the top models – *i.e.*, models that were statistically indistinguishable (ΔAICc<2) from the best model (see footnotes on Tables S8-S11). For Rt, differences among drought years were small (<0.02; Table S8). In contrast, differences among years were larger for Rc and Rs, with coefficients for year highest in 1966, intermediate in 1977, and lowest in 1999.

Tree height, microenvironment, and drought tolerance

Taller trees (based on H in the drought year) showed stronger growth reductions during drought (*i.e.*, lower Rt) and less rebound following drought (*i.e.*, lower Rc and Rs; Table 1; Fig. **3**). Specifically, for Rt, $ln[H]$ appeared, with negative coefficient, in the best model (ΔAICc=0) and all top models when evaluating the three drought years together (Tables S8-S9). The same held true for 1966 individually, but there was no significant effect of $ln[H]$ for 1977 or 1999 individually. For Rc, $ln[H]$ appeared, with negative coefficient, in the best model without a $ln[H] * ln[TWI]$ interaction, for the three drought years together and for 1977, but not for 1966 or 1999. For Rs, again considering the best models without a $ln[H] * ln[TWI]$ interaction, there was a negative effect of $ln[H]$ for the three drought years together and for 1966 and 1977, and a non-significant negative trend in 1999.

Trees in drier microsites showed greater growth declines during drought; *i.e.*, Rt had a significantly negative response to $ln[TWI]$ across all drought years combined, and in 1977 and 1999 individually (Fig. **3**, Table S8-S9). The $ln[H] * ln[TWI]$ interaction was never significant, and had a positive sign in any top Rt models in which it appeared (Tables 1, S8-S9), rejecting the hypothesis that smaller trees (presumably with smaller rooting volume) are more susceptible to drought in microenvironments with a deeper water table. In contrast, $ln[TWI]$ did not appear in any of the best models for Rc or Rs (combined of for individual years), except in interaction with $ln[H]$ (Fig. **3**, Tables S10-S11). Negative $ln[H] * ln[TWI]$ interactions appeared in the best models for both Rc and Rs for all years combined, as well as in one individual year for each (1966 for Rc, 1977 for Rs). This implies a non-significant tendency for small trees to have greater recovery and resilience in wetter microhabitats, but for large trees to have greater recovery and resilience in dry microhabitats.

Species' traits and drought tolerance

Species, as a factor in ANOVA, had significant ($p<0.05$) influence on all traits (WD, LMA, PLA_{dry}, and π_{tlp}), with more significant pairwise differences for WD and PLA_{dry} than for LMA and π_{tlp} (Table 2, Fig. **S4**). Drought tolerance also varied across species, overall and in each drought year (Figs. **4, S7**). Species with overall lowest and highest Rt and Rs were, respectively, *L. tulipifera* (mean Rt = 0.66, mean Rs = 1.04) and *Fagus grandifolia* (mean Rt = 0.99; mean Rs = 1.65). These two species–notably the only two diffuse-porous species in our study–differed significantly from one another in Rt and Rs in each drought year (Fig. **4**).

WD, LMA, and xylem porosity were all poor predictors of drought tolerance (Tables 1, S4-S5). WD and LMA were never significantly associated with Rt, Rc, or Rs in the single-variable tests and were therefore excluded from the full models. Xylem porosity had no significant influence on Rt or Rs in models for all droughts combined (Tables S4, S7). In contrast, Rc was significantly higher in diffuse- and semi-ring porous species than in ring-porous species (Table S6, Fig. **4**).

Drought resistance and resilience, but not recovery, were negatively correlated with PLA_{dry} and π_{tlp} (Fig. **3**; Tables 1, S4-S11). For Rt, PLA_{dry} had a significant influence, with negative

coefficient, in top models for the three droughts combined and for the 1966 drought individually (Fig. **3**; Tables S8-S9). It was also included in some of the top models for 1999 (Tables S8-S9). π_{tlp} was included with a negative coefficient in the best model for the combined droughts scenario and for the 1977 drought individually (Fig. **3**; Table S8), although its influence was not significant at ΔAICc<2. It was also included in some of the top models for 1999 (Tables S8-S9).

Recovery was not significantly correlated with either PLA_{dry} or π_{tlp}. There was only one best Rc model containing one of these terms (π_{tlp} in 1977 drought), but in no instance was one of these terms included in all top models (i.e., at ΔAICc<2).

For Rs, PLA_{dry} was in the best models for the three droughts combined and for the 1966 drought individually, and some of the top models for 1977 and 1999 (Fig. **3**; Table S11); however, its effects were not significant at ΔAICc<2. π_{tlp} was in the best models for the three droughts combined and for 1966 and 1999 individually, and in one of the top models for 1977 (Fig. **3**; Table S11). However, its effects were significant at ΔAICc<2 for 1999 only.

Discussion

Tree height, microenvironment, and leaf drought tolerance traits shaped tree growth responses across three droughts at our study site (Table 1, Fig. **3**). Taller trees had greater exposure to conditions that would promote water loss and heat damage during drought (Fig. **2**), which is one plausible mechanism for their lower drought resistance, recovery, and resilience (Fig. **3**). There was no evidence that greater availability of, or access to, soil water availability increased drought resistance; in contrast, trees in wetter topographic positions had lower Rt (Zuleta et al. 2017; Stovall, Shugart, and Yang 2019), and the larger potential rooting volume of large trees provided no advantage in the drier microenvironments. The negative effect of height on Rt held after accounting for species' traits, which is consistent with recent work finding height had a stronger influence on mortality risk than forest type during drought (Stovall, Shugart, and Yang 2020). Drought tolerance was not consistently linked to species' LMA, WD, or xylem type (ring-

vs. diffuse porous), but was negatively correlated with leaf drought tolerance traits (PLA_{dry}, π_{tlp}). This is the first study to our knowledge linking PLA_{dry} and π_{tlp} to growth reduction during drought. The directions of these responses were consistent across droughts (Table S8), supporting the premise that they were driven by fundamental physiological mechanisms. However, the strengths of each predictor varied across droughts (Fig. **3**; Tables S8-S9), indicating that drought characteristics interact with tree size, microenvironment, and traits to shape which individuals are most affected. These findings advance our knowledge of the factors that make trees vulnerable to stem growth declines during drought and, by extension, likely make them more vulnerable to mortality (Sapes et al. 2019).

The droughts considered here were of a magnitude that has occurred with an average frequency of approximately once every 10-15 years (Fig. **1a**, Helcoski et al. 2019) and had substantial but short-lived impacts on tree growth (Fig. **1**). These droughts were classified as severe ($PDSI$ < -3.0; 1977) or extreme ($PDSI$ < -4.0; 1966, 1999) at our site and have been linked to tree mortality in the eastern United States (Druckenbrod et al. 2019), but were modest compared to the so-called "megadroughts" that have triggered massive tree die-off in other regions (e.g., Allen et al. 2010; Stovall, Shugart, and Yang 2019; Clark et al. 2016). Of the droughts considered here, the 1966 drought, which was preceded by two years of dry conditions (Fig. **S1**), severely stressed a larger portion of trees (Fig. **1b**). The tendency for large trees to have lowest resistance was most pronounced in this drought, consistent with other findings that this physiological response increases with drought severity (Bennett et al. 2015; Stovall, Shugart, and Yang 2019). Across all three droughts, the majority of trees experienced reduced growth, but a substantial portion (e.g., short understory trees, species with drought resistant traits) had increased growth (Figs. **1b, 3**), consistent with prior observations that smaller trees can exhibit increased growth rates during drought (Bennett et al. 2015). Growth rebounded strongly following the droughts, on average exceeding pre-drought growth rates (Fig. **1**), particularly for shorter trees and species with drought-tolerant traits (Figs. **3-4**). It is likely because of the moderate impact of these droughts, along with other factors influencing tree growth (e.g., stand

dynamics), that our best models characterize only a modest amount of variation in *Rt*, *Rc*, and *Rs*: 11-18% for all droughts combined, and 13-30% for individual droughts (Tables S8-S11).

Consistent with studies in other forests worldwide (Bennett et al. 2015), taller trees in this forest exhibited lower drought resistance–and also recovery and resilience–when compared to smaller trees. Mechanistically, this is consistent with, and reinforces, previous findings for a trade-off between the ability of trees to efficiently transport water to great heights and simultaneously maintain strong resistance and resilience to drought-induced embolism (Liu et al. 2019; Olson et al. 2018; Couvreur et al. 2018; Roskilly et al. 2019). Taller trees also face dramatically distinctive microenvironments (Fig. **2**). They are exposed to higher wind speeds and lower humidity (Fig. **2a,b**), resulting in higher evaporative demand. Unlike other temperate forests where modestly cooler understory conditions have been documented (Zellweger et al. 2019), particularly under drier conditions (Davis et al. 2019), we observed no significant variation in air temperatures across the vertical profile (Fig. **2c**). More critically for tree physiology, leaf temperatures can become significantly elevated over air temperature under conditions of high solar radiation and low stomatal conductance (Campbell and Norman 1998; Rey-Sánchez et al. 2016). Under drought, when direct solar radiation tends to be higher (because of less cloud cover) and less water is available for evaporative cooling of the leaves, trees with sun-exposed crowns may not be able to simultaneously maintain leaf temperatures below damaging extremes and avoid drought-induced embolism. Indeed, previous studies have shown lower drought resistance in more exposed trees (Liu and Muller 1993; Suarez, Ghermandi, and Kitzberger 2004; Scharnweber et al. 2019). Unfortunately, collinearity between height and crown exposure in this study (Fig. **2d**) makes it impossible to confidently partition causality. Additional research comparing drought responses of early successional and mature forest stands, along with short and tall isolated trees, would be valuable for more clearly disentangling the roles of tree height and crown exposure.

Belowground, taller trees would tend to have larger root systems (Enquist and Niklas 2002; Hui et al. 2014), but this does not necessarily imply that they have greater access to or reliance on deep soil-water resources that may be critical during drought. While tree size can correlate with

the depth of water extraction (Brum et al. 2019), the linkage is not consistent. Shorter trees can vary broadly in the depth of water uptake (Stahl et al. 2013), and larger trees may allocate more to abundant shallow roots that are beneficial for taking up water from rainstorms (Meinzer et al. 1999). Moreover, reliance on deep soil-water resources can actually prove a liability during severe and prolonged drought, as these can experience more intense water scarcity relative to non-drought conditions (Chitra-Tarak et al. 2018). In any case, the potentially greater access to water did not override the disadvantage conferred by height–and, in fact, greater moisture access in non-drought years (here, higher TWI) appears to make trees more sensitive to drought (Zuleta et al. 2017; Stovall, Shugart, and Yang 2019). This may be because moister habitats would tend to support species and individuals with more mesophytic traits (Bartlett et al. 2016b; Mencuccini 2003; Medeiros et al. 2019), potentially growing to greater heights (e.g., Detto et al. 2013), and these are then more vulnerable when drought occurs. The observed height-sensitivity of Rt, together with the lack of conferred advantage to large stature in drier topographic positions, agrees with the concept that physiological limitations to transpiration under drought shift from soil water availability to the plant-atmosphere interface as forests age (Bretfeld, Ewers, and Hall 2018), such that tall, dominant trees are the most sensitive in mature forests. Again, additional research comparing drought responses across forests with different tree heights and water availability would be valuable for disentangling the relative importance of above- and belowground mechanisms across trees of different size.

The development of tree-ring chronologies for the twelve most dominant tree species at our site (Helcoski et al. 2019; Bourg et al. 2013) provided a sufficient sample size to compare historical drought responses across species (Fig. **4**) and associated traits at a single site (see also Elliott et al. 2015). Our study reinforced current understanding (see Introduction) that WD and LMA are not reliably linked to drought tolerance (Table 1). Contrary to several previous studies in temperate deciduous forests (Friedrichs et al. 2009; Elliott et al. 2015; Kannenberg et al. 2019), we did not find an association between xylem porosity and drought resistance or resilience, as the two diffuse-porous species, *L.* and *F. grandifolia*, were at opposite ends of the Rt spectrum (Fig. **4**). While the low Rt of *L. tulipifera* is consistent with other studies (Elliott et al. 2015), the

high Rt of *F. grandifolia* contrasts with studies identifying diffuse porous species in general (Elliott et al. 2015; Kannenberg et al. 2019), and the genus *Fagus* in particular (Friedrichs et al. 2009), as drought sensitive. There are two potential explanations for this discrepancy. First, other traits can and do override the influence of xylem porosity on drought resistance. Ring-porous species are restricted mainly to temperate deciduous forests, while highly drought-tolerant diffuse-porous species exist in other biomes (Wheeler, Baas, and Rodgers 2007). *F. grandifolia* had intermediate π_{tlp} and low PLA_{dry} (Fig. **S4**), which would have contributed to its drought tolerance (Fig. **3**; see discussion below), in concordance with studies identifying *Fagus* species as intermediate in drought tolerance (Vitasse et al. 2019; Pretzsch, Schütze, and Biber 2018). A second explanation of why *F. grandifolia* trees at this particular site had higher Rt and Rs is that the sampled individuals, reflective of the population within the plot, are generally shorter and in less-dominant canopy positions compared to most other species (Fig. **S4**). The species, which is highly shade-tolerant, also has deep crowns (Anderson-Teixeira, McGarvey, et al. 2015), implying that a lower proportion of leaves would be affected by harsher microclimatic conditions at the top of the canopy under drought (Fig. **2**). Thus, the high Rt and Rs of the sampled *F. grandifolia* population can be explained by a combination of fairly drought-resistant leaf traits, shorter stature, and a buffered microenvironment.

Concerted measurement of tree-rings and leaf drought tolerance traits of emerging importance in published literature (Scoffoni et al. 2014; Bartlett et al. 2016a; Medeiros et al. 2019) allowed novel insights into the role of drought tolerance traits in shaping drought response. The finding that PLA_{dry} and π_{tlp} can be useful for predicting drought responses of tree growth (Fig. **3**; Table 1) is both novel and consistent with previous studies linking these traits to habitat and drought tolerance. Previous studies have demonstrated that π_{tlp} and PLA_{dry} are physiologically meaningful traits linked to species distribution along moisture gradients (Maréchaux et al. 2015; Fletcher et al. 2018; Medeiros et al. 2019; Simeone et al. 2019; Rosas et al. 2019; Zhu et al. 2018), and our findings indicate that these traits also influence drought responses. Furthermore, the observed linkage of π_{tlp} to Rt in this forest aligns with observations in the Amazon that π_{tlp} is higher in drought-intolerant than drought-tolerant plant functional type.

Further, it adds support to the idea that this trait is useful for categorizing and representing species' drought responses in models (Powell et al. 2017). Because both PLA_{dry} and π_{tlp} can be measured relatively easily (Bartlett et al. 2012; Scoffoni et al. 2014), they hold promise for predicting drought growth responses across diverse forests. The importance of predicting drought responses from species traits increases with tree species diversity; whereas it is feasible to study drought responses for all dominant species in most boreal and temperate forests (e.g., this study), this becomes difficult to impossible for diverse tropical forests where most species do not form annual rings (but see Schöngart et al. 2017 for a review of progress in tropical dendroecology). A full linkage of drought tolerance traits to drought responses would be invaluable for forecasting how little-known species and whole forests will respond to future droughts (Christoffersen et al. 2016; Powell et al. 2017).

As climate change drives increasing drought in many of the world's forests (Trenberth et al. 2014; Intergovernmental Panel on Climate Change 2015), the fate of forests and their climate feedbacks will be shaped by the biophysical and physiological drivers observed here. Our results show that taller, more exposed trees and species with less drought-tolerant leaf traits will be most affected in terms of both growth during the drought year and subsequent growth. Survival is linked to resistance and resilience (DeSoto et al. 2020; Gessler et al. 2020), implying it may be influenced by the same factors. Indeed, while no link between PLA_{dry} or π_{tlp} on drought survival has been established (but see Powers et al. 2020), taller trees have lower survival (Bennett et al. 2015; Stovall, Shugart, and Yang 2019). As climate change-driven droughts affect forests worldwide, there is likely to be a shift from mature forests with tall, buffering trees to forests with a shorter overall stature (McDowell et al. 2020). At this point, species whose drought tolerance relies in part on existence within a buffered microenvironment (e.g., *F. grandifolia*) could in turn become more susceptible. Here, the relative importance of tree height *per se* versus crown exposure becomes crucial, shaping whether the dominant trees of shorter canopies are significantly more drought tolerant because of their shorter stature, or whether high exposure makes them as vulnerable as the taller trees of the former canopy. Studies disentangling the influence of height and exposure on drought

tolerance will be critical to answering this question. Ultimately, distributions of tree heights and drought tolerance traits across broad moisture gradients suggest that forests exposed to more drought will shift towards shorter stature and be dominated by species with more drought-tolerant traits (Liu et al. 2019; Bartlett et al. 2016a; Zhu et al. 2018). Our study helps to elucidate the mechanisms behind these patterns, opening the door for more accurate forecasting of forest responses to future drought.

Acknowledgements

We especially thank the numerous researchers who helped to collect the data used here, in particular Jennifer C. McGarvey, Jonathan R. Thompson, and Victoria Meakem for original collection and processing of cores. Thanks also to Camila D. Medeiros for guidance on leaf drought tolerance and functional trait measurements, Edward Brzostek's lab for collaboration on leaf sampling, and Maya Prestipino for data collection. This manuscript was improved based on helpful reviews by Mark Olson and three anonymous reviewers. Funding for the establishment of the SCBI ForestGEO Large Forest Dynamics Plot was provided by the Smithsonian-led Forest Global Earth Observatory (ForestGEO), the Smithsonian Institution, and the HSBC Climate Partnership. This study was funded by ForestGEO, a Virginia Native Plant Society grant to KAT and AJT, and support from the Harvard Forest and National Science Foundation which supports the PalEON project (NSF EF-1241930) for NP.

Author Contribution

KJA-T, IRM, and AJT designed the research. Tree-ring chronologies were developed by RH under guidance of AJT, KAT, and NP. Trait data were collected by IRM and JZ under guidance of NK, KAT, and LS. Other plot data were collected by NAB in coordination with WJM and by IRM and AELS under guidance of EBG-A and KJA-T. Data analyses were performed by IRM under guidance of KJA-T and VH. KJA-T and IRM interpreted the results. IRM and KJA-T wrote the first draft of manuscript, and all authors contributed to revisions.

Data and code availability

All data, code, and results are available through the SCBI-ForestGEO organization on GitHub (https://github.com/SCBI-ForestGEO: SCBI-ForestGEO-Data and McGregor_climate-sensitivity-variation repositories), with static versions corresponding to data and analyses presented here archived in Zenodo (DOIs: 10.5281/zenodo.4070038 and *[TBD]*, respectively. Full ForestGEO census data for SCBI are available through the ForestGEO data portal (www.forestgeo.si.edu).

ORCID

Ian R. McGregor: 0000-0002-5763-021X

Norbert Kunert: 0000-0002-5602-6221

Alan J. Tepley: 0000-0002-5701-9613

Erika B. Gonzalez-Akre: 0000-0001-8305-6672

Valentine Herrmann: 0000-0002-4519-481X

Joseph Zailaa: 0000-0001-9103-190X

Atticus E.L. Stovall: 0000-0001-9512-3318

Norman A. Bourg: 0000-0002-7443-1992

William J. McShea: 0000-0002-8102-0200

Neil Pederson: 0000-0003-3830-263X

Lawren Sack: 0000-0002-7009-7202

Kristina J. Anderson-Teixeira: 0000-0001-8461-9713

Supplementary Information

Table S1. Monthly Palmer Drought Severity Index (PDSI), and its rank among all years between 1950 and 2009 for focal droughts.

Table S2. Species-specific bark thickness regression equations.

Table S3. Species-specific height regression equations.

Table S4. Individual tests of species traits as drivers of drought resistance, where Rt is used as the response variable.

Table S5. Individual tests of species traits as drivers of drought resistance, where Rt_{ARIMA} is used as the response variable.

Table S6. Individual tests of species traits as drivers of drought recovery (Rc).

Table S7. Individual tests of species traits as drivers of drought resilience (Rs).

Table S8. Summary of top full models for each drought instance, where Rt is used as the response variable.

Table S9. Summary of top models for each drought instance, where Rt_{ARIMA} is used as the response variable.

Table S10. Summary of top models for each drought instance, where Rc is used as the response variable.

Table S11. Summary of top models for each drought instance, where Rs is used as the response variable.

Figure S1. Time series of Palmer Drought Severity Index (PDSI) for the 2 years prior and after each focal drought.

Figure S2. Map of ForestGEO plot showing topographic wetness index and location of cored trees.

Figure S3. Distribution of reconstructed tree heights across drought years.

Figure S4. Distribution of independent variables by species.

Figure S5. Comparison of Rt and Rt_{ARIMA} results, with residuals, for each drought scenario

Figure S6. Density plot of Recovery (Rc) values for each focal year.

Figure S7. Drought recovery, Rc, across species for the three focal droughts.

Methods S1. Further Package Citations

References

Abrams, Marc D. 1990. “Adaptations and Responses to Drought in Quercus Species of North America.” *Tree Physiology* 7 (1-2-3-4): 227–38. https://doi.org/10.1093/treephys/7.1-2-3-4.227.

Allen, Craig D., David D. Breshears, and Nate G. McDowell. 2015. “On Underestimation of Global Vulnerability to Tree Mortality and Forest Die-Off from Hotter Drought in the Anthropocene.” *Ecosphere* 6 (8). https://doi.org/10.1890/ES15-00203.1.

Allen, Craig D., Alison K. Macalady, Haroun Chenchouni, Dominique Bachelet, Nate McDowell, Michel Vennetier, Thomas Kitzberger, et al. 2010. “A Global Overview of Drought and Heat-Induced Tree Mortality Reveals Emerging Climate Change Risks for Forests.” *Forest Ecology and Management*, Adaptation of Forests and Forest Management to Changing Climate, 259 (4): 660–84. https://doi.org/10.1016/j.foreco.2009.09.001.

Anderegg, William R. L., Tamir Klein, Megan Bartlett, Lawren Sack, Adam F. A. Pellegrini, Brendan Choat, and Steven Jansen. 2016. “Meta-Analysis Reveals That Hydraulic Traits Explain Cross-Species Patterns of Drought-Induced Tree Mortality Across the Globe.” *Proceedings of the National Academy of Sciences* 113 (18): 5024–9. https://doi.org/10.1073/pnas.1525678113.

Anderson-Teixeira, Kristina J., Stuart J. Davies, Amy C. Bennett, Erika B. Gonzalez-Akre, Helene C. Muller-Landau, S. Joseph Wright, Kamariah Abu Salim, et al. 2015. “CTFS-ForestGEO: A Worldwide Network Monitoring Forests in an Era of Global Change.” *Global Change Biology* 21 (2): 528–49. https://doi.org/10.1111/gcb.12712.

Anderson-Teixeira, Kristina J., Jennifer C. McGarvey, Helene C. Muller-Landau, Janice Y. Park, Erika B. Gonzalez-Akre, Valentine Herrmann, Amy C. Bennett, et al. 2015. “Size-Related Scaling of Tree Form and Function in a Mixed-Age Forest.” *Functional Ecology* 29 (12): 1587–1602. https://doi.org/10.1111/1365-2435.12470.

Bartlett, Megan K., Tamir Klein, Steven Jansen, Brendan Choat, and Lawren Sack. 2016a. “The Correlations and Sequence of Plant Stomatal, Hydraulic, and Wilting Responses to Drought.”

Proceedings of the National Academy of Sciences 113 (46): 13098–13103. https://doi.org/10.1073/pnas.1604088113.

Bartlett, Megan K., Christine Scoffoni, Rico Ardy, Ya Zhang, Shanwen Sun, Kunfang Cao, and Lawren Sack. 2012. "Rapid Determination of Comparative Drought Tolerance Traits: Using an Osmometer to Predict Turgor Loss Point." *Methods in Ecology and Evolution* 3 (5): 880–88. https://doi.org/10.1111/j.2041-210X.2012.00230.x.

Bartlett, M. K., Y. Zhang, J. Yang, N. Kreidler, S.-W. Sun, L. Lin, Y.-H. Hu, K.-F. Cao, and L. Sack. 2016b. "Drought Tolerance as a Driver of Tropical Forest Assembly: Resolving Spatial Signatures for Multiple Processes." *Ecology* 97 (2): 503–14. https://doi.org/10.1890/15-0468.1.

Bates, Douglas, Martin Maechler, Ben Bolker, and Steven Walker. 2019. *Lme4: Linear Mixed-Effects Models Using 'Eigen' and S4*. https://CRAN.R-project.org/package=lme4.

Bennett, Amy C., Nathan G. McDowell, Craig D. Allen, and Kristina J. Anderson-Teixeira. 2015. "Larger Trees Suffer Most During Drought in Forests Worldwide." *Nature Plants* 1 (10): 15139. https://doi.org/10.1038/nplants.2015.139.

Beven, K. J., and M. J. Kirkby. 1979. "A Physically Based, Variable Contributing Area Model of Basin Hydrology / Un Modèle à Base Physique de Zone d'appel Variable de L'hydrologie Du Bassin Versant." *Hydrological Sciences Bulletin* 24 (1): 43–69. https://doi.org/10.1080/02626667909491834.

Bonan, Gordon B. 2008. "Forests and Climate Change: Forcings, Feedbacks, and the Climate Benefits of Forests." *Science* 320 (5882): 1444–9. https://doi.org/10.1126/science.1155121.

Bourg, Norman A., William J. McShea, Jonathan R. Thompson, Jennifer C. McGarvey, and Xiaoli Shen. 2013. "Initial Census, Woody Seedling, Seed Rain, and Stand Structure Data for the SCBI SIGEO Large Forest Dynamics Plot." *Ecology* 94 (9): 2111–2. https://doi.org/10.1890/13-0010.1.

Bretfeld, Mario, Brent E. Ewers, and Jefferson S. Hall. 2018. "Plant Water Use Responses Along Secondary Forest Succession During the 2015–2016 El Niño Drought in Panama." *New Phytologist* 219 (3): 885–99. https://doi.org/10.1111/nph.15071.

Brewer, Mark J., Adam Butler, and Susan L. Cooksley. 2016. "The Relative Performance of AIC, AICC and BIC in the Presence of Unobserved Heterogeneity." *Methods in Ecology and Evolution* 7 (6): 679–92. https://doi.org/10.1111/2041-210X.12541.

Brum, Mauro, Matthew A. Vadeboncoeur, Valeriy Ivanov, Heidi Asbjornsen, Scott Saleska, Luciana F. Alves, Deliane Penha, et al. 2019. "Hydrological Niche Segregation Defines Forest Structure and Drought Tolerance Strategies in a Seasonal Amazon Forest." *Journal of Ecology* 107 (1): 318–33. https://doi.org/10.1111/1365-2745.13022.

Campbell, Gaylon S., and John M. Norman. 1998. *An Introduction to Environmental Biophysics*. Vol. 2nd. New York: Springer.

Chitra-Tarak, Rutuja, Laurent Ruiz, Handanakere S. Dattaraja, M. S. Mohan Kumar, Jean Riotte, Hebbalalu S. Suresh, Sean M. McMahon, and Raman Sukumar. 2018. "The Roots of the Drought: Hydrology and Water Uptake Strategies Mediate Forest-Wide Demographic Response to Precipitation." *Journal of Ecology* 106 (4): 1495–1507. https://doi.org/10.1111/1365-2745.12925.

Christoffersen, Bradley O., Manuel Gloor, Sophie Fauset, Nikolaos M. Fyllas, David R. Galbraith, Timothy R. Baker, Bart Kruijt, et al. 2016. "Linking Hydraulic Traits to Tropical Forest Function in a Size-Structured and Trait-Driven Model (TFS V.1-Hydro)." *Geoscientific Model Development* 9 (11): 4227–55. https://doi.org/https://doi.org/10.5194/gmd-9-4227-2016.

Clark, James S., Louis Iverson, Christopher W. Woodall, Craig D. Allen, David M. Bell, Don C. Bragg, Anthony W. D'Amato, et al. 2016. "The Impacts of Increasing Drought on Forest Dynamics, Structure, and Biodiversity in the United States." *Global Change Biology* 22 (7): 2329–52. https://doi.org/10.1111/gcb.13160.

Condit, Richard. 1998. *Tropical Forest Census Plots: Methods and Results from Barro Colorado Island, Panama and a Comparison with Other Plots*. Berlin, Heidelberg: Springer Berlin Heidelberg. https://doi.org/10.1007/978-3-662-03664-8.

Cook, Benjamin I., Toby R. Ault, and Jason E. Smerdon. 2015. "Unprecedented 21st Century Drought Risk in the American Southwest and Central Plains." *Science Advances* 1 (1): e1400082. https://doi.org/10.1126/sciadv.1400082.

Couvreur, Valentin, Glenn Ledder, Stefano Manzoni, Danielle A. Way, Erik B. Muller, and Sabrina E. Russo. 2018. "Water Transport Through Tall Trees: A Vertically Explicit, Analytical Model of Xylem Hydraulic Conductance in Stems." *Plant, Cell & Environment* 41 (8): 1821–39. https://doi.org/10.1111/pce.13322.

Dai, Aiguo, Tianbao Zhao, and Jiao Chen. 2018. "Climate Change and Drought: A Precipitation and Evaporation Perspective." *Current Climate Change Reports* 4 (3): 301–12. https://doi.org/10.1007/s40641-018-0101-6.

Davis, Kimberley T., Solomon Z. Dobrowski, Zachary A. Holden, Philip E. Higuera, and John T. Abatzoglou. 2019. "Microclimatic Buffering in Forests of the Future: The Role of Local Water Balance." *Ecography* 42 (1): 1–11. https://doi.org/10.1111/ecog.03836.

DeSoto, Lucía, Maxime Cailleret, Frank Sterck, Steven Jansen, Koen Kramer, Elisabeth M. R. Robert, Tuomas Aakala, et al. 2020. "Low Growth Resilience to Drought Is Related to Future Mortality Risk in Trees." *Nature Communications* 11 (1): 545. https://doi.org/10.1038/s41467-020-14300-5.

Detto, Matteo, Helene C. Muller-Landau, Joseph Mascaro, and Gregory P. Asner. 2013. "Hydrological Networks and Associated Topographic Variation as Templates for the Spatial Organization of Tropical Forest Vegetation." *PLOS ONE* 8 (10). https://doi.org/10.1371/journal.pone.0076296.

Druckenbrod, Daniel L., Dario Martin-Benito, David A. Orwig, Neil Pederson, Benjamin Poulter, Katherine M. Renwick, and Herman H. Shugart. 2019. "Redefining Temperate Forest Responses

to Climate and Disturbance in the Eastern United States: New Insights at the Mesoscale." *Global Ecology and Biogeography* 28 (5): 557–75. https://doi.org/10.1111/geb.12876.

Elliott, Katherine J., Chelcy F. Miniat, Neil Pederson, and Stephanie H. Laseter. 2015. "Forest Tree Growth Response to Hydroclimate Variability in the Southern Appalachians." *Global Change Biology* 21 (12): 4627–41. https://doi.org/10.1111/gcb.13045.

Enquist, Brian J., and Karl J. Niklas. 2002. "Global Allocation Rules for Patterns of Biomass Partitioning in Seed Plants." *Science* 295 (5559): 1517–20. https://doi.org/10.1126/science.1066360.

Farrell, Claire, Christopher Szota, and Stefan K. Arndt. 2017. "Does the Turgor Loss Point Characterize Drought Response in Dryland Plants?" *Plant, Cell & Environment* 40 (8): 1500–1511. https://doi.org/10.1111/pce.12948.

Fletcher, Leila R., Hongxia Cui, Hilary Callahan, Christine Scoffoni, Grace P. John, Megan K. Bartlett, Dylan O. Burge, and Lawren Sack. 2018. "Evolution of Leaf Structure and Drought Tolerance in Species of Californian Ceanothus." *American Journal of Botany* 105 (10): 1672–87. https://doi.org/10.1002/ajb2.1164.

Friedlingstein, P., P. Cox, R. Betts, L. Bopp, W. von Bloh, V. Brovkin, P. Cadule, et al. 2006. "Climate–Carbon Cycle Feedback Analysis: Results from the C4MIP Model Intercomparison." *Journal of Climate* 19 (14): 3337–53. https://doi.org/10.1175/JCLI3800.1.

Friedrichs, Dagmar A., Valerie Trouet, Ulf Büntgen, David C. Frank, Jan Esper, Burkhard Neuwirth, and Jörg Löffler. 2009. "Species-Specific Climate Sensitivity of Tree Growth in Central-West Germany." *Trees* 23 (4): 729. https://doi.org/10.1007/s00468-009-0315-2.

Gessler, Arthur, Alessandra Bottero, John Marshall, and Matthias Arend. 2020. "The Way Back: Recovery of Trees from Drought and Its Implication for Acclimation." *New Phytologist*, May. https://doi.org/10.1111/nph.16703.

Gillerot, Loïc, David I. Forrester, Alessandra Bottero, Andreas Rigling, and Mathieu Lévesque. 2020. "Tree Neighbourhood Diversity Has Negligible Effects on Drought Resilience of European Beech, Silver Fir and Norway Spruce." *Ecosystems*, April. https://doi.org/10.1007/s10021-020-00501-y.

Gonzalez-Akre, Erika, Kristina Anderson-Teixeira, Ian McGregor, Valentine Herrmann, and RHelcoski. 2019. "SCBI-ForestGEO/SCBI-ForestGEO-Data: First Official Release." Zenodo. https://doi.org/10.5281/ZENODO.2649302.

Gonzalez-Akre, Erika, Victoria Meakem, Cheng-Yin Eng, Alan J. Tepley, Norman A. Bourg, William McShea, Stuart J. Davies, and Kristina Anderson-Teixeira. 2016. "Patterns of Tree Mortality in a Temperate Deciduous Forest Derived from a Large Forest Dynamics Plot." *Ecosphere* 7 (12). https://doi.org/10.1002/ecs2.1595.

Greenwood, Sarah, Paloma Ruiz-Benito, Jordi Martínez-Vilalta, Francisco Lloret, Thomas Kitzberger, Craig D. Allen, Rod Fensham, et al. 2017. "Tree Mortality Across Biomes Is Promoted by Drought Intensity, Lower Wood Density and Higher Specific Leaf Area." *Ecology Letters* 20 (4): 539–53. https://doi.org/10.1111/ele.12748.

Guerfel, Mokhtar, Olfa Baccouri, Dalenda Boujnah, Wided Chaïbi, and Mokhtar Zarrouk. 2009. "Impacts of Water Stress on Gas Exchange, Water Relations, Chlorophyll Content and Leaf Structure in the Two Main Tunisian Olive (Olea Europaea L.) Cultivars." *Scientia Horticulturae* 119 (3): 257–63. https://doi.org/10.1016/j.scienta.2008.08.006.

Harris, I., P. D. Jones, T. J. Osborn, and D. H. Lister. 2014. "Updated High-Resolution Grids of Monthly Climatic Observations – the CRU TS3.10 Dataset." *International Journal of Climatology* 34 (3): 623–42. https://doi.org/10.1002/joc.3711.

Helcoski, Ryan, Alan J. Tepley, Neil Pederson, Jennifer C. McGarvey, Victoria Meakem, Valentine Herrmann, Jonathan R. Thompson, and Kristina J. Anderson-Teixeira. 2019. "Growing Season Moisture Drives Interannual Variation in Woody Productivity of a Temperate Deciduous Forest." *New Phytologist* 223 (3): 1204–16. https://doi.org/10.1111/nph.15906.

Hoffmann, William A., Renée M. Marchin, Pamela Abit, and On Lee Lau. 2011. "Hydraulic Failure and Tree Dieback Are Associated with High Wood Density in a Temperate Forest Under Extreme Drought." *Global Change Biology* 17 (8): 2731–42. https://doi.org/10.1111/j.1365-2486.2011.02401.x.

Hollister, Jeffrey. 2018. *Elevatr: Access Elevation Data from Various Apis*. https://CRAN.R-project.org/package=elevatr.

Hui, Dafeng, Jun Wang, Weijun Shen, Xuan Le, Philip Ganter, and Hai Ren. 2014. "Near Isometric Biomass Partitioning in Forest Ecosystems of China." *PLOS ONE* 9 (1): e86550. https://doi.org/10.1371/journal.pone.0086550.

Hyndman, Rob, George Athanasopoulos, Christoph Bergmeir, Gabriel Caceres, Leanne Chhay, Mitchell O'Hara-Wild, Fotios Petropoulos, Slava Razbash, Earo Wang, and Farah Yasmeen. 2020. *Forecast: Forecasting Functions for Time Series and Linear Models*. https://CRAN.R-project.org/package=forecast.

Intergovernmental Panel on Climate Change. 2015. *Climate Change 2014: Impacts, Adaptation and Vulnerability: Working Group II Contribution to the IPCC Fifth Assessment Report. Volume 2 Volume 2*. https://doi.org/10.1017/CBO9781107415386.

Jennings, S. B., N. D. Brown, and D. Sheil. 1999. "Assessing Forest Canopies and Understorey Illumination: Canopy Closure, Canopy Cover and Other Measures." *Forestry: An International Journal of Forest Research* 72 (1): 59–74. https://doi.org/10.1093/forestry/72.1.59.

Kannenberg, Steven A., Kimberly A. Novick, M. Ross Alexander, Justin T. Maxwell, David J. P. Moore, Richard P. Phillips, and William R. L. Anderegg. 2019. "Linking Drought Legacy Effects Across Scales: From Leaves to Tree Rings to Ecosystems." *Global Change Biology* 25 (9): 2978–92. https://doi.org/10.1111/gcb.14710.

Katabuchi, Masatoshi. 2019. *LeafArea: Rapid Digital Image Analysis of Leaf Area*. https://CRAN.R-project.org/package=LeafArea.

Kennedy, Daniel, Sean Swenson, Keith W. Oleson, David M. Lawrence, Rosie Fisher, Antonio Carlos Lola da Costa, and Pierre Gentine. 2019. "Implementing Plant Hydraulics in the Community Land Model, Version 5." *Journal of Advances in Modeling Earth Systems* 11 (2): 485–513. https://doi.org/10.1029/2018MS001500.

Koike, T., M. Kitao, Y. Maruyama, S. Mori, and T. T. Lei. 2001. "Leaf Morphology and Photosynthetic Adjustments Among Deciduous Broad-Leaved Trees Within the Vertical Canopy Profile." *Tree Physiology* 21 (12-13): 951–58. https://doi.org/10.1093/treephys/21.12-13.951.

Kunert, Norbert, Luiza Maria T. Aparecido, Stefan Wolff, Niro Higuchi, Joaquim dos Santos, Alessandro Carioca de Araujo, and Susan Trumbore. 2017. "A Revised Hydrological Model for the Central Amazon: The Importance of Emergent Canopy Trees in the Forest Water Budget." *Agricultural and Forest Meteorology* 239 (May): 47–57. https://doi.org/10.1016/j.agrformet.2017.03.002.

Larjavaara, Markku, and Helene C. Muller-Landau. 2013. "Measuring Tree Height: A Quantitative Comparison of Two Common Field Methods in a Moist Tropical Forest." *Methods in Ecology and Evolution* 4 (9): 793–801. https://doi.org/10.1111/2041-210X.12071.

Liu, Hui, Sean M. Gleason, Guangyou Hao, Lei Hua, Pengcheng He, Guillermo Goldstein, and Qing Ye. 2019. "Hydraulic Traits Are Coordinated with Maximum Plant Height at the Global Scale." *Science Advances* 5 (2). https://doi.org/10.1126/sciadv.aav1332.

Liu, Yan, and Robert N. Muller. 1993. "Effect of Drought and Frost on Radial Growth of Overstory and Undesrstory Stems in a Deciduous Forest." *The American Midland Naturalist* 129 (1): 19–25. https://doi.org/10.2307/2426431.

Lloret, Francisco, Eric G. Keeling, and Anna Sala. 2011. "Components of Tree Resilience: Effects of Successive Low-Growth Episodes in Old Ponderosa Pine Forests." *Oikos* 120 (12): 1909–20. https://doi.org/10.1111/j.1600-0706.2011.19372.x.

Lunch, Claire, Christine Laney, Nathan Mietkiewicz, Eric Sokol, Kaelin Cawley, and NEON (National Ecological Observatory Network). 2020. *NeonUtilities: Utilities for Working with Neon Data*. https://CRAN.R-project.org/package=neonUtilities.

Maréchaux, Isabelle, Megan K. Bartlett, Lawren Sack, Christopher Baraloto, Julien Engel, Emilie Joetzjer, and Jérôme Chave. 2015. "Drought Tolerance as Predicted by Leaf Water Potential at Turgor Loss Point Varies Strongly Across Species Within an Amazonian Forest." *Functional Ecology* 29 (10): 1268–77. https://doi.org/10.1111/1365-2435.12452.

Maréchaux, Isabelle, Laurent Saint-André, Megan K. Bartlett, Lawren Sack, and Jérôme Chave. 2020. "Leaf Drought Tolerance Cannot Be Inferred from Classic Leaf Traits in a Tropical Rainforest." *Journal of Ecology* 108 (3): 1030–45. https://doi.org/10.1111/1365-2745.13321.

Martin-Benito, Dario, and Neil Pederson. 2015. "Convergence in Drought Stress, but a Divergence of Climatic Drivers Across a Latitudinal Gradient in a Temperate Broadleaf Forest." *Journal of Biogeography* 42 (5): 925–37. https://doi.org/10.1111/jbi.12462.

Martin-Benito, Dario, and Neil Pederson. 2015. "Convergence in Drought Stress, but a Divergence of Climatic Drivers Across a Latitudinal Gradient in a Temperate Broadleaf Forest." *Journal of Biogeography* 42 (5): 925–37. https://doi.org/10.1111/jbi.12462.

Mazerolle, Marc J., and portions of code contributed by Dan Linden. 2019. *AICcmodavg: Model Selection and Multimodel Inference Based on (Q)AIC(c)*. https://CRAN.R-project.org/package=AICcmodavg.

McDowell, Nate G., Craig D. Allen, Kristina Anderson-Teixeira, Brian H. Aukema, Ben Bond-Lamberty, Louise Chini, James S. Clark, et al. 2020. "Pervasive Shifts in Forest Dynamics in a Changing World." *Science* 368 (6494). https://doi.org/10.1126/science.aaz9463.

McDowell, Nate G., Barbara J. Bond, Lee T. Dickman, Michael G. Ryan, and David Whitehead. 2011. "Relationships Between Tree Height and Carbon Isotope Discrimination." In *Size- and Age-Related Changes in Tree Structure and Function*, edited by Frederick C. Meinzer, Barbara

Lachenbruch, and Todd E. Dawson, 255–86. Tree Physiology. Dordrecht: Springer Netherlands. https://doi.org/10.1007/978-94-007-1242-3_10.

McDowell, Nathan G., and Craig D. Allen. 2015. "Darcy's Law Predicts Widespread Forest Mortality Under Climate Warming." *Nature Climate Change* 5 (7): 669–72. https://doi.org/10.1038/nclimate2641.

Meakem, Victoria, Alan J. Tepley, Erika B. Gonzalez-Akre, Valentine Herrmann, Helene C. Muller-Landau, S. Joseph Wright, Stephen P. Hubbell, Richard Condit, and Kristina J. Anderson-Teixeira. 2018. "Role of Tree Size in Moist Tropical Forest Carbon Cycling and Water Deficit Responses." *New Phytologist* 219 (3): 947–58. https://doi.org/10.1111/nph.14633.

Medeiros, Camila D., Christine Scoffoni, Grace P. John, Megan K. Bartlett, Faith Inman-Narahari, Rebecca Ostertag, Susan Cordell, Christian Giardina, and Lawren Sack. 2019. "An Extensive Suite of Functional Traits Distinguishes Hawaiian Wet and Dry Forests and Enables Prediction of Species Vital Rates." *Functional Ecology* 33 (4): 712–34. https://doi.org/10.1111/1365-2435.13229.

Meinzer, F. C., José Luis Andrade, Guillermo Goldstein, N. Michele Holbrook, Jaime Cavelier, and S. Joseph Wright. 1999. "Partitioning of Soil Water Among Canopy Trees in a Seasonally Dry Tropical Forest." *Oecologia* 121 (3): 293–301. https://doi.org/10.1007/s004420050931.

Mencuccini, M. 2003. "The Ecological Significance of Long-Distance Water Transport: Short-Term Regulation, Long-Term Acclimation and the Hydraulic Costs of Stature Across Plant Life Forms." *Plant, Cell & Environment* 26 (1): 163–82. https://doi.org/10.1046/j.1365-3040.2003.00991.x.

Merlin, Morgane, Thomas Perot, Sandrine Perret, Nathalie Korboulewsky, and Patrick Vallet. 2015. "Effects of Stand Composition and Tree Size on Resistance and Resilience to Drought in Sessile Oak and Scots Pine." *Forest Ecology and Management* 339 (March): 22–33. https://doi.org/10.1016/j.foreco.2014.11.032.

Metcalfe, Peter, Keith Beven, and Jim Freer. 2018. *Dynatopmodel: Implementation of the Dynamic Topmodel Hydrological Model*. https://CRAN.R-project.org/package=dynatopmodel.

NEON. 2018. "National Ecological Observatory Network. 2016, 2017, 2018. Data Products: DP1.00001.001, DP1.00098.001, DP1.00002.001. Provisional Data Downloaded from Http://Data.neonscience.org/ in May 2019. Battelle, Boulder, CO, USA."

Olson, Mark E., Tommaso Anfodillo, Julieta A. Rosell, Giai Petit, Alan Crivellaro, Sandrine Isnard, Calixto León-Gómez, Leonardo O. Alvarado-Cárdenas, and Matiss Castorena. 2014. "Universal Hydraulics of the Flowering Plants: Vessel Diameter Scales with Stem Length Across Angiosperm Lineages, Habits and Climates." *Ecology Letters* 17 (8): 988–97. https://doi.org/10.1111/ele.12302.

Olson, Mark E., Diana Soriano, Julieta A. Rosell, Tommaso Anfodillo, Michael J. Donoghue, Erika J. Edwards, Calixto León-Gómez, et al. 2018. "Plant Height and Hydraulic Vulnerability to Drought and Cold." *Proceedings of the National Academy of Sciences* 115 (29): 7551–6. https://doi.org/10.1073/pnas.1721728115.

Olson, Mark, Julieta A. Rosell, Cecilia Martínez-Pérez, Calixto León-Gómez, Alex Fajardo, Sandrine Isnard, María Angélica Cervantes-Alcayde, et al. 2020. "Xylem Vessel-Diameter–Shoot-Length Scaling: Ecological Significance of Porosity Types and Other Traits." *Ecological Monographs* 90 (3). https://doi.org/10.1002/ecm.1410.

Phillips, N. G., M. G. Ryan, B. J. Bond, N. G. McDowell, T. M. Hinckley, and J. Čermák. 2003. "Reliance on Stored Water Increases with Tree Size in Three Species in the Pacific Northwest." *Tree Physiology* 23 (4): 237–45. https://doi.org/10.1093/treephys/23.4.237.

Powell, Thomas L., James K. Wheeler, Alex A. R. de Oliveira, Antonio Carlos Lola da Costa, Scott R. Saleska, Patrick Meir, and Paul R. Moorcroft. 2017. "Differences in Xylem and Leaf Hydraulic Traits Explain Differences in Drought Tolerance Among Mature Amazon Rainforest Trees." *Global Change Biology* 23 (10): 4280–93. https://doi.org/10.1111/gcb.13731.

Powers, Jennifer S., German Vargas G, Timothy J. Brodribb, Naomi B. Schwartz, Daniel Pérez-Aviles, Chris M. Smith-Martin, Justin M. Becknell, et al. 2020. "A Catastrophic Tropical Drought Kills Hydraulically Vulnerable Tree Species." *Global Change Biology* 26 (5): 3122–33. https://doi.org/10.1111/gcb.15037.

Pretzsch, Hans, Gerhard Schütze, and Peter Biber. 2018. "Drought Can Favour the Growth of Small in Relation to Tall Trees in Mature Stands of Norway Spruce and European Beech." *Forest Ecosystems* 5 (1): 20. https://doi.org/10.1186/s40663-018-0139-x.

R Core Team. 2019. *R: A Language and Environment for Statistical Computing*. Vienna, Austria: R Foundation for Statistical Computing. https://www.R-project.org/.

Rey-Sánchez, A. Camilo, Martijn Slot, Juan M. Posada, and Kaoru Kitajima. 2016. "Spatial and Seasonal Variation in Leaf Temperature Within the Canopy of a Tropical Forest." *Climate Research* 71 (1): 75–89. https://doi.org/10.3354/cr01427.

Rosas, Teresa, Maurizio Mencuccini, Josep Barba, Hervé Cochard, Sandra Saura-Mas, and Jordi Martínez-Vilalta. 2019. "Adjustments and Coordination of Hydraulic, Leaf and Stem Traits Along a Water Availability Gradient." *New Phytologist* 223 (2): 632–46. https://doi.org/10.1111/nph.15684.

Roskilly, Beth, Eric Keeling, Sharon Hood, Arnaud Giuggiola, and Anna Sala. 2019. "Conflicting Functional Effects of Xylem Pit Structure Relate to the Growth-Longevity Trade-Off in a Conifer Species." *Proceedings of the National Academy of Sciences* 116 (30): 15282–7. https://doi.org/10.1073/pnas.1900734116.

Ryan, Michael G., Nathan Phillips, and Barbara J. Bond. 2006. "The Hydraulic Limitation Hypothesis Revisited." *Plant, Cell & Environment* 29 (3): 367–81. https://doi.org/10.1111/j.1365-3040.2005.01478.x.

Sapes, Gerard, Beth Roskilly, Solomon Dobrowski, Marco Maneta, William R. L. Anderegg, Jordi Martinez-Vilalta, and Anna Sala. 2019. "Plant Water Content Integrates Hydraulics and Carbon

Depletion to Predict Drought-Induced Seedling Mortality." *Tree Physiology* 39 (8): 1300–1312. https://doi.org/10.1093/treephys/tpz062.

Scharnweber, Tobias, Lisa Heinze, Roberto Cruz-García, Marieke van der Maaten-Theunissen, and Martin Wilmking. 2019. "Confessions of Solitary Oaks: We Grow Fast but We Fear the Drought." *Dendrochronologia* 55 (June): 43–49. https://doi.org/10.1016/j.dendro.2019.04.001.

Scholz, Fabian G., Nathan G. Phillips, Sandra J. Bucci, Frederick C. Meinzer, and Guillermo Goldstein. 2011. "Hydraulic Capacitance: Biophysics and Functional Significance of Internal Water Sources in Relation to Tree Size." In *Size- and Age-Related Changes in Tree Structure and Function*, edited by Frederick C. Meinzer, Barbara Lachenbruch, and Todd E. Dawson, 341–61. Tree Physiology. Dordrecht: Springer Netherlands. https://doi.org/10.1007/978-94-007-1242-3_13.

Schöngart, Jochen, Achim Bräuning, Ana Carolina Maioli Campos Barbosa, Claudio Sergio Lisi, and Juliano Morales de Oliveira. 2017. "Dendroecological Studies in the Neotropics: History, Status and Future Challenges." In *Dendroecology: Tree-Ring Analyses Applied to Ecological Studies*, edited by Mariano M. Amoroso, Lori D. Daniels, Patrick J. Baker, and J. Julio Camarero, 35–73. Ecological Studies. Cham: Springer International Publishing. https://doi.org/10.1007/978-3-319-61669-8_3.

Scoffoni, Christine, Christine Vuong, Steven Diep, Hervé Cochard, and Lawren Sack. 2014. "Leaf Shrinkage with Dehydration: Coordination with Hydraulic Vulnerability and Drought Tolerance." *Plant Physiology* 164 (4): 1772–88. https://doi.org/10.1104/pp.113.221424.

Simeone, Caelan, Marco P. Maneta, Zachary A. Holden, Gerard Sapes, Anna Sala, and Solomon Z. Dobrowski. 2019. "Coupled Ecohydrology and Plant Hydraulics Modeling Predicts Ponderosa Pine Seedling Mortality and Lower Treeline in the US Northern Rocky Mountains." *New Phytologist* 221 (4): 1814–30. https://doi.org/10.1111/nph.15499.

Slette, Ingrid J., Alison K. Post, Mai Awad, Trevor Even, Arianna Punzalan, Sere Williams, Melinda D. Smith, and Alan K. Knapp. 2019. "How Ecologists Define Drought, and Why We

Should Do Better." *Global Change Biology* 25 (10): 3193–3200. https://doi.org/10.1111/gcb.14747.

Stahl, Clément, Bruno Hérault, Vivien Rossi, Benoit Burban, Claude Bréchet, and Damien Bonal. 2013. "Depth of Soil Water Uptake by Tropical Rainforest Trees During Dry Periods: Does Tree Dimension Matter?" *Oecologia* 173 (4): 1191–1201. https://doi.org/10.1007/s00442-013-2724-6.

Stovall, Atticus E. L., Kristina J. Anderson-Teixeira, and Herman H. Shugart. 2018a. "Terrestrial LiDAR-Derived Non-Destructive Woody Biomass Estimates for 10 Hardwood Species in Virginia." *Data in Brief* 19 (August): 1560–9. https://doi.org/10.1016/j.dib.2018.06.046.

———. 2018b. "Assessing Terrestrial Laser Scanning for Developing Non-Destructive Biomass Allometry." *Forest Ecology and Management* 427 (November): 217–29. https://doi.org/10.1016/j.foreco.2018.06.004.

Stovall, Atticus E. L., Herman H. Shugart, and Xi Yang. 2020. "Reply to 'Height-Related Changes in Forest Composition Explain Increasing Tree Mortality with Height During an Extreme Drought'." *Nature Communications* 11 (1): 3401. https://doi.org/10.1038/s41467-020-17214-4.

Stovall, Atticus E. L., Herman Shugart, and Xi Yang. 2019. "Tree Height Explains Mortality Risk During an Intense Drought." *Nature Communications* 10 (1): 1–6. https://doi.org/10.1038/s41467-019-12380-6.

Suarez, Maria Laura, Luciana Ghermandi, and Thomas Kitzberger. 2004. "Factors Predisposing Episodic Drought-Induced Tree Mortality in Nothofagus– Site, Climatic Sensitivity and Growth Trends." *Journal of Ecology* 92 (6): 954–66. https://doi.org/10.1111/j.1365-2745.2004.00941.x.

Sørensen, R., U. Zinko, and J. Seibert. 2006. "On the Calculation of the Topographic Wetness Index: Evaluation of Different Methods Based on Field Observations." *Hydrology and Earth System Sciences* 10 (1): 101–12. https://doi.org/https://doi.org/10.5194/hess-10-101-2006.

Trenberth, Kevin E., Aiguo Dai, Gerard van der Schrier, Philip D. Jones, Jonathan Barichivich, Keith R. Briffa, and Justin Sheffield. 2014. "Global Warming and Changes in Drought." *Nature Climate Change* 4 (1): 17–22. https://doi.org/10.1038/nclimate2067.

Trugman, A. T., M. Detto, M. K. Bartlett, D. Medvigy, W. R. L. Anderegg, C. Schwalm, B. Schaffer, and S. W. Pacala. 2018. "Tree Carbon Allocation Explains Forest Drought-Kill and Recovery Patterns." *Ecology Letters* 21 (10): 1552–60. https://doi.org/10.1111/ele.13136.

Vitasse, Yann, Alessandra Bottero, Maxime Cailleret, Christof Bigler, Patrick Fonti, Arthur Gessler, Mathieu Lévesque, et al. 2019. "Contrasting Resistance and Resilience to Extreme Drought and Late Spring Frost in Five Major European Tree Species." *Global Change Biology* 25 (11): 3781–92. https://doi.org/10.1111/gcb.14803.

Wheeler, E. A., P. Baas, and S. Rodgers. 2007. "Variations in Dieot Wood Anatomy: A Global Analysis Based on the Insidewood Database." *IAWA Journal* 28 (3): 229–58. https://doi.org/10.1163/22941932-90001638.

Zach, Alexandra, Bernhard Schuldt, Sarah Brix, Viviana Horna, Heike Culmsee, and Christoph Leuschner. 2010. "Vessel Diameter and Xylem Hydraulic Conductivity Increase with Tree Height in Tropical Rainforest Trees in Sulawesi, Indonesia." *Flora - Morphology, Distribution, Functional Ecology of Plants* 205 (8): 506–12. https://doi.org/10.1016/j.flora.2009.12.008.

Zellweger, Florian, David Coomes, Jonathan Lenoir, Leen Depauw, Sybryn L. Maes, Monika Wulf, Keith J. Kirby, et al. 2019. "Seasonal Drivers of Understorey Temperature Buffering in Temperate Deciduous Forests Across Europe." *Global Ecology and Biogeography* 28 (12): 1774–86. https://doi.org/10.1111/geb.12991.

Zhu, Shi-Dan, Ya-Jun Chen, Qing Ye, Peng-Cheng He, Hui Liu, Rong-Hua Li, Pei-Li Fu, Guo-Feng Jiang, and Kun-Fang Cao. 2018. "Leaf Turgor Loss Point Is Correlated with Drought Tolerance and Leaf Carbon Economics Traits." *Tree Physiology* 38 (5): 658–63. https://doi.org/10.1093/treephys/tpy013.

Zuleta, Daniel, Alvaro Duque, Dairon Cardenas, Helene C. Muller-Landau, and Stuart J. Davies. 2017. “Drought-Induced Mortality Patterns and Rapid Biomass Recovery in a Terra Firme Forest in the Colombian Amazon.” *Ecology* 98 (10): 2538–46. https://doi.org/10.1002/ecy.1950.

Hypotheses & Specific Predictions	Prediction supported? recent non-drought conditions	Resistance (Rt)	Recovery (Rc)	Resilience (Rs)	Results
Tree size and microenvironment					
Across the forest vertical profile, taller trees are exposed to higher evaporative demand.					
Taller trees experience higher wind speeds during the peak growing season months.	yes				Fig. 2
Taller trees experience lower humidity during the peak growing season months.	yes				Fig. 2
Taller trees experience higher air temperatures during the peak growing season months.	no				Fig. 2
Taller trees have more sun-exposed crowns.	yes				Fig. 2
At least within the forest setting, taller trees are less drought tolerant.					
Drought tolerance decreases with height (H).		yes	yes	yes	Fig. 4; Tables S8-S11
Smaller trees (lower root volume) in drier microhabitats have lower drought tolerance.					
There is a negative interactive effect between H and topographic wetness index.		(no)	(yes)	(yes)	Tables S8-S11
Species traits					
Species' traits – particularly leaf drought tolerance traits – predict drought tolerance.					
Wood density correlates (positively or negatively) to drought tolerance.		-	-	-	Tables S4-S7
Leaf mass per area correlates positively to drought tolerance.		-	-	-	Tables S4-S7
Ring-porous species have higher drought tolerance than diffuse- or semi-ring- porous.		-	no	-	Tables S4-S7

Percent loss leaf area upon desiccation correlates negatively with drought tolerance.	yes	(yes)	(yes)	Fig. 4; Tables S8-S11
Water potential at turgor loss correlates negatively with drought tolerance.	(yes)	(yes)	(yes)	Fig. 4; Tables S8-S11

Table 1. Summary of hypotheses, corresponding specific predictions, and results.

Parentheses indicate that the prediction was supported by at least one but not all of the top models (Tables S8, S10, S11). Dash symbols indicate that the response was not significant (Tables S4, S6, S7).

Table 2. Overview of analyzed species, listed in order of their relative contributions to woody stem productivity ($ANPPstem$) in the plot, along with numbers and sizes sampled, and species traits.

			contemporary DBH (cm)		species traits (mean ± se)				
species	*% $ANPP_{stem}$*	n trees*	mean	range	*WD (g cm^{-3})*	*LMA (g cm^{-2})*	xylem porosity	π_{tlp} (MPa)	*PLA_{dry} (%)*
Liriodendron tulipifera L. (LITU)	47.1	98	36.9	10 - 100.4	0.4 ± 0.03	46.9 ± 12.4	diffuse	-1.92 ± 0.17	19.6 ± 2.06
Quercus alba L. (QUAL)	10.7	61	47.2	11.4 - 79.1	0.61 ± 0.02	75.8 ± 11.1	ring	-2.58 ± 0.08	8.52 ± 0.37
Quercus rubra L. (QURU)	10.1	69	54.9	11.1 - 148	0.62 ± 0.02	71.1 ± 6.70	ring	-2.64 ± 0.28	11.0 ± 0.84
Quercus velutina Lam. (QUVE)	7.8	77	54.1	16.0 - 114.2	0.65 ± 0.04	48.7 ± 3.30	ring	-2.39 ± 0.15	13.42 ± 0.84
Quercus montana L. (QUPR)	4.8	59	42.3	10.5 - 87.2	0.61 ± 0.01	71.8 ± 40.2	ring	-2.36 ± 0.09	11.75 ± 1.37
Fraxinus americana L. (FRAM)	3.8	62	35.4	6.4 - 94.7	0.56 ± 0.01	43.3 ± 4.78	ring	-2.1 ± 0.36	13.06 ± 1.06
Carya glabra (Mill.) Sweet (CAGL)	3.7	31	31.4	9.8 - 98.5	0.62 ± 0.04	42.8 ± 0.94	ring	-2.13 ± 0.50	21.09 ± 5.48
Juglans nigra L. (JUNI)	2.1	31	48.1	24.2 - 87	1.09 ± 0.09	72.1 ± 7.10	semi-ring	-2.76 ± 0.21	24.64 ± 8.72
Carya cordiformis (Wangenh.) K. Koch (CACO)	2	13	27.2	10.7 - 61.5	0.83 ± 0.10	45.9 ± 15.6	ring	-2.13 ± 0.45	17.22 ± 2.25
Carya tomentosa (Lam. ex Poir.) Nutt. (CATO)	2	13	21	12.1 - 32.2	0.83	45.4	ring	-2.2	16.56
Fagus grandifolia Ehrh. (FAGR)	1.5	80	23.5	11.2 - 107.2	0.62 ± 0.03	30.7 ± 4.94	diffuse	-2.57	9.45 ± 1.25
Carya ovalis (Wangenh.) Sarg. (CAOVL)	1.1	23	35.3	14.9 - 66.0	0.96 ± 0.33	47.6 ± 3.95	ring	-2.48 ± 0.04	14.8 ± 6.34

Variable abbreviations are as in Table 3. DBH measurements are from the most recent ForestGEO census in 2018 (live trees) or tree mortality censuses in 2016 and 2017 (trees cored dead).

Table 3. Summary of dependent and independent variables in our statistical models of drought tolerance, along with units, definitions, and sample sizes.

variable	symbol	units	description	category	n_{RT}*	n_{Rc}	n_{Rs}
Dependent variables							
drought resistance	*Rt*	-	ratio of basal area increment (BAI) during drought year to mean BAI of the 5 years prior.	-	1623	-	-
	Rt_{ARIMA}	-	ratio of BAI during drought year to BAI predicted by ARIMA model.	-	1654	-	-
drought recovery	*Rc*	-	ratio of mean BAI for 5 years after drought to BAI during drought year.	-	-	1557	-
drought resilience	*Rs*	-	ratio of mean BAI for 5 years after drought to mean BAI for 5 years before drought.	-	-	-	1570
Independent variables							
drought year	*Y*	-	year of drought	1966	513	491	495
				1977	543	524	523
				1999	567	542	552
height	*H*	m	estimated H in drought year	-	-	-	-
topographic wetness index	*TWI*	-	steady-state wetness index based on slope and upstream contributing area	-	-	-	-
Species' traits							
wood density	*WD*	g cm^{-3}	dry mass of a unit volume of fresh wood	-	-	-	-
leaf mass per area	*LMA*	kg m^{-2}	ratio of leaf dry mass to fresh leaf area	-	-	-	-

xylem porosity	-	vessel arrangement in xylem	ring (R)	1106	1079		1088
			semi-ring (SR)	81	73		78
			diffuse (D)	436	405		404
turgor loss point	π_{tlp}	MPa	water potential at which leaves wilt	-	-	-	-
percent loss area	PLA_{dry}	%	percent loss of leaf area upon dessication	-	-	-	-

Sample sizes are after removal of outliers. Dashes for sample sizes of independent variables indicate that the variable was available for all records. Xylem porosity sample sizes are sums across all drought years.

*Sample sizes of independent variables refer to the Rt model.

Figure Legends

Figure 1. Climate and species-level growth responses over our study period, highlighting the three focal droughts (a) and community-wide growth resistance, *Rt* (b), and resilience, *Rs* (c). Time series plot (a) shows peak growing season (May-August) climate conditions and residual chronologies for each species (see Table 3 for codes). PET and PRE data were obtained from the Climatic Research Unit high-resolution gridded dataset (CRU TS v.4.01; Harris et al. 2014). Focal droughts are indicated by dashed lines, and shading indicates the pre- and post- drought periods used in calculations of the resistance metric. Figure modified from Helcoski *et al.* (2019). Density plots (b-c) show the distribution of *Rt* and *Rs* values for each drought. See Fig. S6 for parallel plot for recovery (*Rc*).

Figure 2. Contemporary height profiles in sun exposure and growing season microclimate under non-drought conditions. Shown are average (± SD) of daily maxima and minima of (a) wind speed, (b) relative humidity (*RH*), and (c) air temperature (T_{air}) averaged over each month of the peak growing season (May-August) from 2016-2018. In these plots, heights are slightly offset for visualization purposes. Asterisks indicate significant differences between the top and bottom of the height profile. Also shown is (d) tree heights by 2018 crown position, with letters indicating significance groupings. In all plots, the dashed horizontal line indicates the 95th percentile of tree heights in the ForestGEO plot.

Figure 3. Visualization of top statistical models for drought resistance (*Rt*), recovery (*Rc*), and resilience (*Rs*) for all droughts combined and for each individual drought year. For cases where the best model includes a DBH x TWI interaction (*Rc* in all droughts and 1966, *Rs* in all droughts and 1977), we plot the best model without the interaction. Visualization of the best mixed effects model per drought scenario was created by the *visreg* package in R, and confidence intervals were defined via bootstrapping in the *bootpredictlme4* package. Model coefficients are given in Tables S8 and S10-11. Descriptions of variables (e.g. *ln*[*H*] can be found in Table 3.

Figure 4. Drought resistance, *Rt* (a), and resilience, *Rs* (b) across species for the three focal droughts. Species codes are given in Table 2. Shaded boxes represent the interquartile range, with horizontal line at median, whiskers represent the range within 2.7 SD, and dots represent outliers. The horizontal dotted line at y=1 represents no change in growth between the five years prior to drought and the drought year (*Rt*) or the five years following the drought (*Rs*). Letters illustrate significance groupings per year (colored and ordered, top to bottom, 1966, 1977, 1999). That is, a group of species with the same letter above their boxplot (e.g. "b") are statistically different from species in another group (e.g. "a"). Letter groupings do not transfer across variables *Rt* and *Rs*. See Fig. S7 for parallel plot for recovery (*Rc*). Analysis conducted using *agricolae* package in R. Descriptions of variables (e.g. *ln*[*H*]) can be found in Table 3

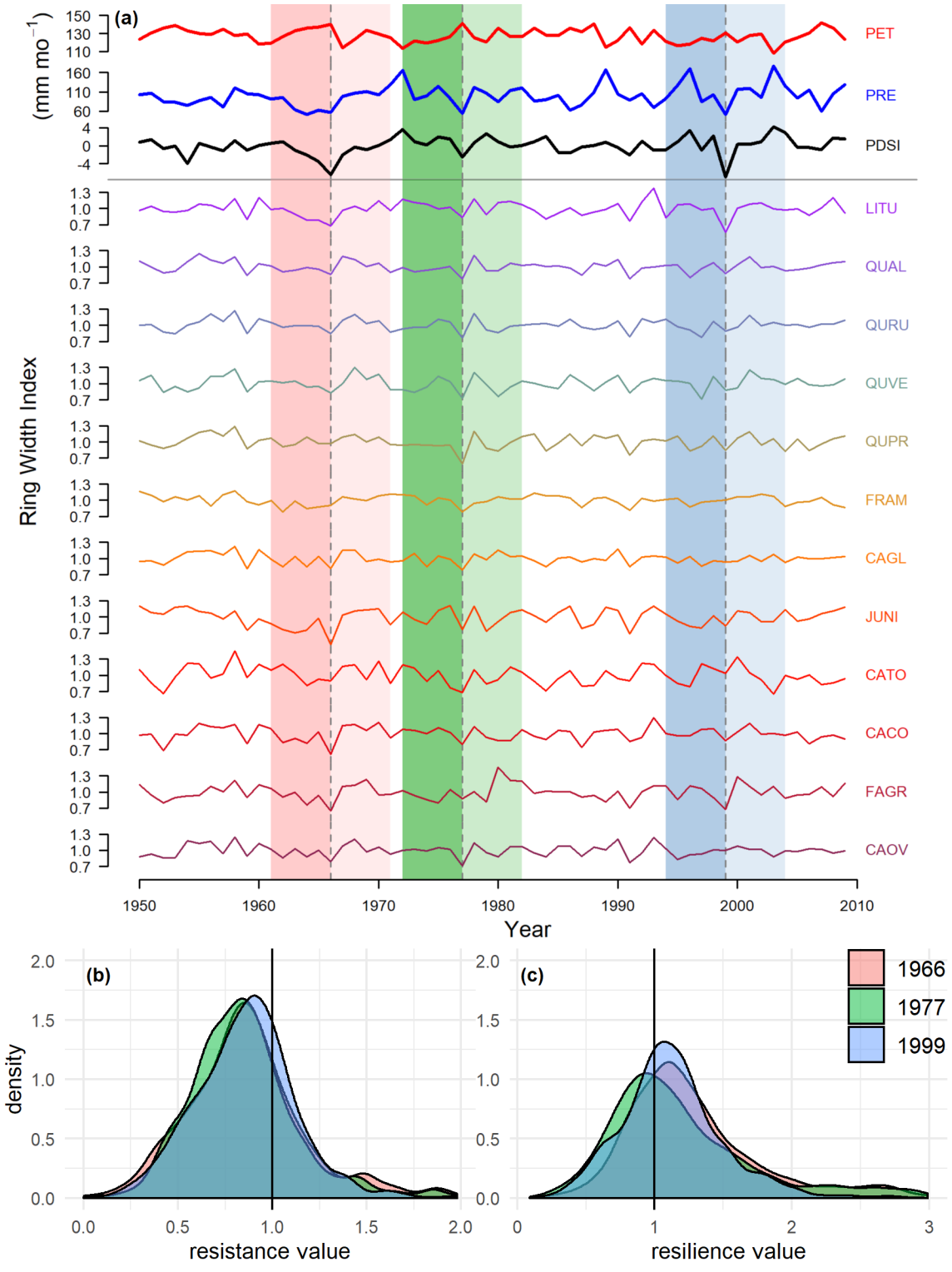

nph_16996_f1.png

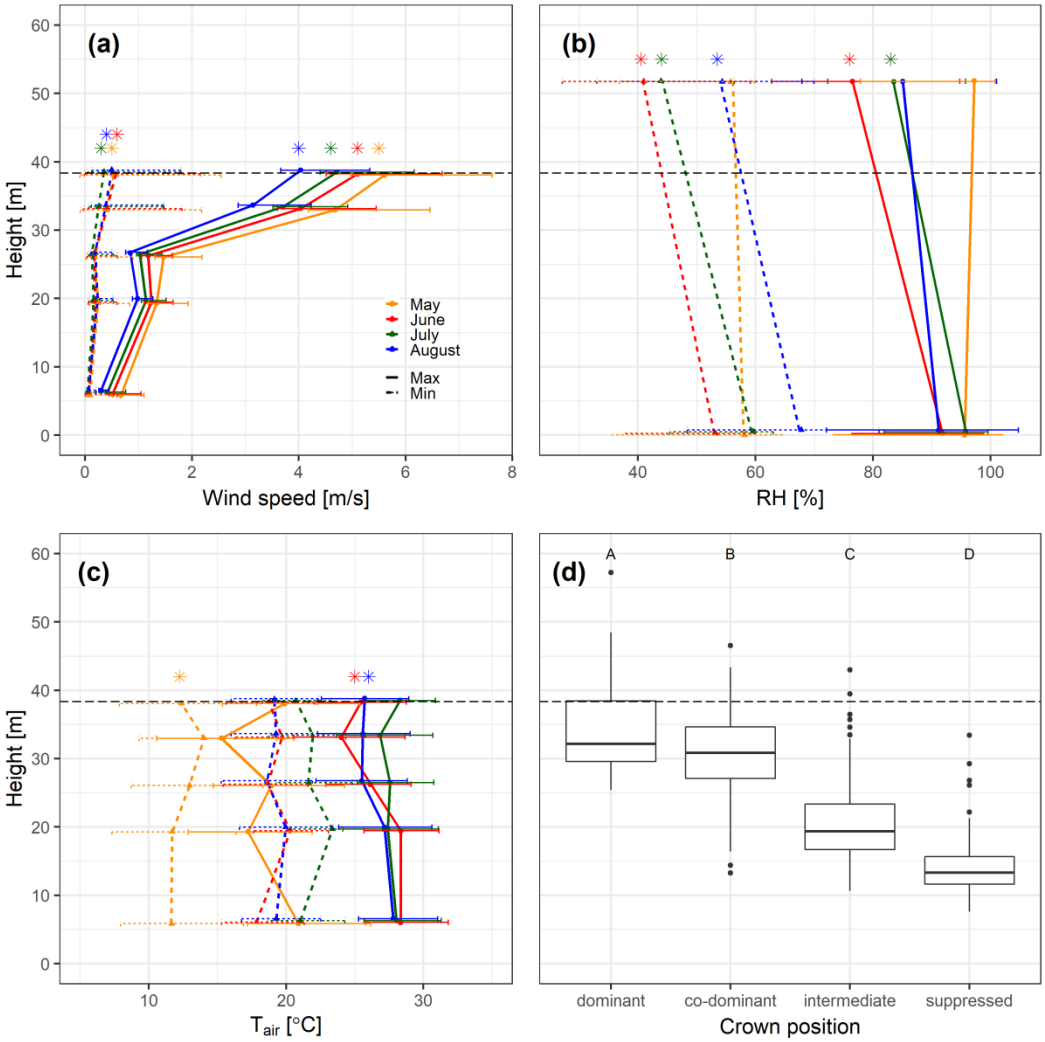

nph_16996_f2.png

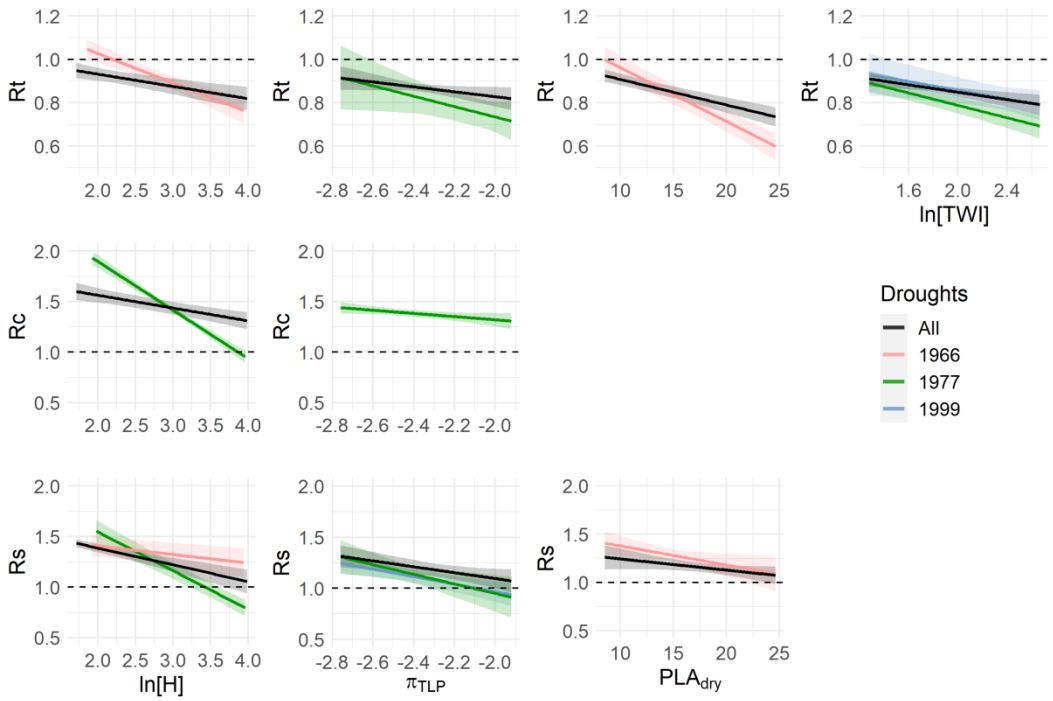

nph_16996_f3.png

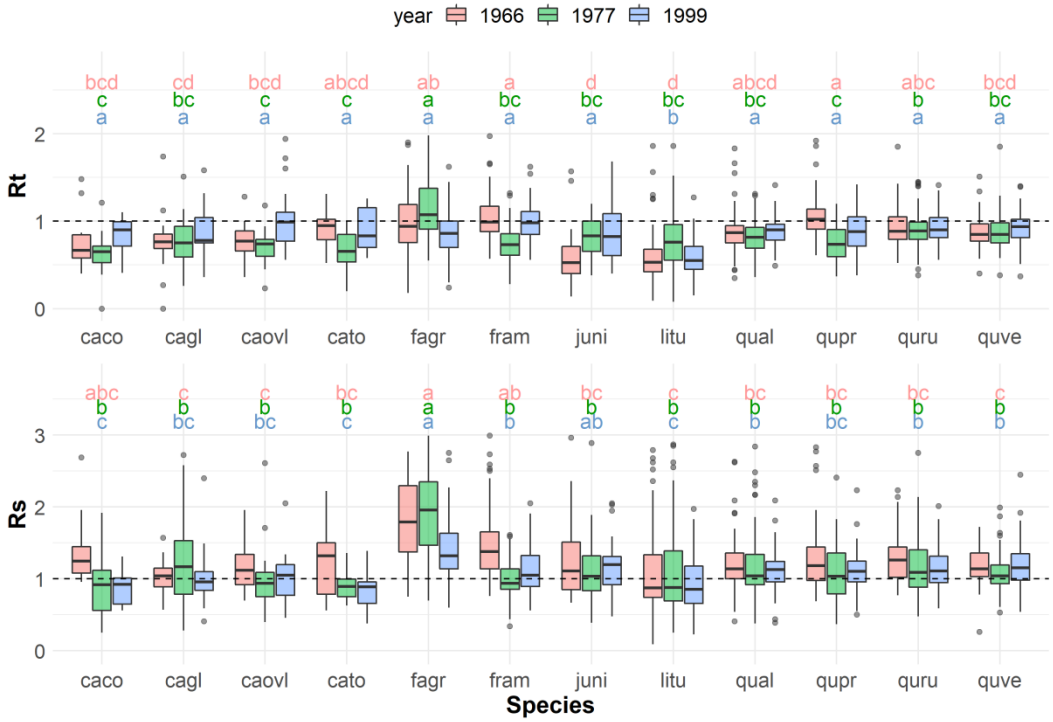

nph_16996_f4.png